Integrated Engineering–Economic Analysis for Multihazard Damage and Loss Assessment

Mehrshad Amini, S.M.ASCE[1]; Hwayoung Jeon[2]; Dylan R. Sanderson, S.M.ASCE[3]; Daniel T. Cox, M.ASCE[4]; Andre R. Barbosa, A.M.ASCE[5]; and Harvey Cutler[6]

Abstract: This paper presents a methodology to evaluate the direct and general equilibrium losses for a testbed community subjected to a megathrust earthquake and tsunami hazard originating in the Cascadia Subduction Zone. The testbed community studied consists of buildings for all residential and commercial sectors in the economy. A fragility analysis and functionality model are applied to estimate the direct damage and losses of these buildings at the parcel level. The process relies on Monte Carlo simulations (MCS) that propagate uncertainties from the hazards through to the damage and loss models. A computable general equilibrium (CGE) model is used to assess aggregated general equilibrium losses to the community. As an important mitigation strategy, seismic retrofit reduces the direct loss to building functionality and general equilibrium losses. Results show that the vulnerability of economic sectors depends on the hazard type, hazard intensity, economic zone, and building type, and the risks vary with the recurrence interval. The highest risks are associated with 500-year and 1,000-year mean recurrence intervals for joint seismic–tsunami hazards, respectively. Results from assessing different design alternatives show that whereas retrofitting all buildings to the highest code level considered results in the lowest losses, retrofitting only commercial buildings can be an efficient retrofit option for enhancing community resilience when controlling for costs. Last, a sensitivity analysis shows that losses and associated risks are sensitive to the definition of building functionality, which highlights the necessity for a common definition of building functionality when performing vulnerability analyses. **DOI: 10.1061/JITSE4.ISENG-2229.**

Author keywords: Community resilience; Computable general equilibrium model (CGE); Economic losses; Mitigation strategy; Multihazards; Seismic retrofit.

Introduction

Natural hazards can threaten communities and negatively impact the built and socioeconomic environments by creating direct damage to buildings and direct capital stock losses and general equilibrium losses, such as those occurring from business interruption and production deficits, as well as employment and real household income losses. Over the last 60 years, it has been estimated that natural hazards have caused general equilibrium losses of $1.2 trillion in the US (CEMHS 2020). Many studies have indicated that general equilibrium losses can exceed direct losses, particularly for vulnerable communities with lower levels of resilience (PDNA 2010; Bocchini et al. 2014). General equilibrium losses show an increasing trend over recent years due to various factors such as climate change, population growth, urban development, and the age of the built infrastructure (Rappaport and Sachs 2003; Liu 2014; Lin and Shullman 2017). Although general equilibrium losses constitute a significant portion of the total losses, an accurate estimate can be challenging due to several factors, including large-scale impacts, complex systems, and the lack of data standards (NRC 1999; Tirasirichai 2007; Gall et al. 2011; Rose and Lim 2002). Nonetheless, an accurate estimate of the total losses and associated risks can help policymakers evaluate the effectiveness of potential mitigation and emergency response strategies and thus better inform community decisions (Meyer et al. 2013; Newman et al. 2017).

Several studies have focused on the assessment of direct damage and losses due to natural hazards to physical infrastructures, including buildings (e.g., Wang et al. 2018; Pilkington 2019), transportation systems (e.g., Sun et al. 2020; Burns et al. 2021), water systems (e.g., Guidotti et al. 2016; Joshi and Mohagheghi 2021), electric power systems (e.g., Ouyang and Duenas-Osorio 2014; Ma et al. 2020), oil and gas networks (e.g., Ouyang and Wang 2015; Ameri and van de Lindt 2019), and associated interdependencies (e.g., Zhang et al. 2016; Attary et al. 2019; Kameshwar et al. 2019; Sanderson et al. 2021b). Generally, the initial damage assessment is achieved by using fragility curves to estimate the direct damage and losses. At the same time, functionality and restoration models are incorporated to characterize the community's postdisaster recovery level. In this regard, additional studies have contributed to developing quantitative methods for the resilience assessment of physical

[1]Postdoctoral Scholar, School of Civil and Construction Engineering, Oregon State Univ., Corvallis, OR 97331 (corresponding author). ORCID: https://orcid.org/0000-0003-1854-0737. Email: mehrshad.amini@oregonstate.edu

[2]Postdoctoral Scholar, Dept. of Economics, Colorado State Univ., Fort Collins, CO 80523. Email: Hwayoung.Jeon@colostate.edu

[3]Ph.D. Student, School of Civil and Construction Engineering, Oregon State Univ., Corvallis, OR 97331. ORCID: https://orcid.org/0000-0002-4443-7074. Email: sanderdy@oregonstate.edu

[4]CH2M Hill Professor in Civil Engineering, School of Civil and Construction Engineering, Oregon State Univ., Corvallis, OR 97331. Email: Dan.Cox@oregonstate.edu

[5]Professor, School of Civil and Construction Engineering, Oregon State Univ., Corvallis, OR 97331. Email: Andre.Barbosa@oregonstate.edu

[6]Professor, Dept. of Economics, Colorado State Univ., Fort Collins, CO 80523. ORCID: https://orcid.org/0000-0002-4176-9815. Email: harvey.cutler@colostate.edu

Note. This manuscript was submitted on July 29, 2022; approved on August 3, 2023; published online on September 26, 2023. Discussion period open until February 26, 2024; separate discussions must be submitted for individual papers. This paper is part of the ***Journal of Infrastructure Systems***, © ASCE, ISSN 1076-0342.

infrastructures considering single or multiple hazards with associated uncertainties (e.g., Chang and Shinozuka 2004; Schultz and Smith 2016; Carey et al. 2019; Kameshwar et al. 2019; Sanderson et al. 2021a, 2022). However, general equilibrium losses due to natural hazards have not been broadly addressed as a resilience metric, particularly at the community level, because it requires modeling the interactions among physical, social, and economic systems (Bocchini et al. 2014; Masoomi et al. 2018; Roohi et al. 2021). Consequently, this potential gap can result in inaccurate community vulnerability assessments, particularly concerning social and economic systems.

Ellingwood et al. (2016) developed a resilience assessment methodology for the Centerville Virtual Community testbed, which includes interactions among physical infrastructures, natural hazards, and population demographics to identify the impact of natural hazards on the community resilience metrics. Furthermore, Cutler et al. (2016) integrated infrastructure damage into computable general equilibrium (CGE) models to evaluate the effect of seismic hazards on the built environment and subsequent impacts on the economy, such as losses to domestic supply and household income. Rose et al. (2016) used CGE analysis to estimate the economic impacts of port cargo disruptions due to a tsunami in Southern California by modeling the economy as a series of interconnected supply chains. They indicated that resilience strategies can significantly reduce both direct and total economic losses by 80%–85%. Chen et al. (2018) proposed a spatially integrated engineering–economic model to assess the vulnerability of a regional economic system to a hypothetical tsunami event. In this study, fragility functions were applied to estimate the physical damage to each economic sector at the parcel level. Then, damage probabilities (serving as the input shocks) were used as inputs to the CGE model to assess economic impacts at the county level. Sensitivity analysis results indicated that a high-resolution engineering–economic model at the parcel level significantly affects the outputs and can potentially improve the assessment of economic losses due to tsunami hazards at the regional level because the intensity of the hazard can significantly fluctuate over a short distance. Attary et al. (2020) developed a dynamic CGE model for the city of Joplin, Missouri, to evaluate the recovery path from a tornado that severely impacted the community in 2011. They reported that delaying external financial assistance such as insurance or governmental support can lead to adverse outcomes for the community. Rosenheim et al. (2019) integrated the engineering–social data by probabilistically coupling the household characteristics to housing units to predict the household dislocation due to a hypothetical earthquake scenario. The method was applied to Seaside, Oregon, a coastal community near the Cascadia Subduction Zone (CSZ) with a local population of over 6,000 people, which is the same testbed used for this study. Wang et al. (2021) proposed a methodology using the CGE model developed in Attary et al. (2020) to investigate the effect of tornado infrastructure damage on population dislocation and the local economy. They also studied the effect of various tornado retrofit strategies on socioeconomic metrics at the community level and found that more advanced retrofit methods result in lower economic losses and less population dislocation. Recently, Wang et al. (2022) extended the methodology to evaluate how various building retrofit levels affect the selected community resilience goals impacted by the tornado. They concluded that although the building retrofit reduces economic losses, the minimum level of building retrofit strongly depends on selected resilience goals and tornado hazard intensity. For example, the household dislocation and employment metrics control the retrofit level for tornados at the routine-level (EF2) and design-level (EF3) hazard intensity, respectively. In terms of the validity of CGE model results, Zhou and Chen (2021) found that the output of the CGE model in disaster impact assessments is sensitive to factors such as modeling mechanisms, type of model, and data. They suggested that using a spatial CGE model helps to improve the model by capturing both heterogeneous characteristics of the natural hazard and the effects of interregional economic activities. In addition, the authors argued that introducing economic resilience into the model provides a more realistic assessment of outcomes.

The previous literature review has identified several research gaps, particularly in the assessment of general equilibrium losses due to natural hazards within the community. First, to the authors' best knowledge, there is no study investigating the effect of multihazard earthquake and tsunamis on general equilibrium losses. Second, most of the previous studies adopted a deterministic, scenario-based approach for the hazard analysis, including historical or hypothetical scenarios. Although useful for understanding some aspects, scenario-based approaches lack the ability to identify the probabilistic nature of economic losses. Therefore, a risk-based analysis including a reasonable range of hazard intensities associated with a recurrence interval should be employed to better understand the effect of natural hazards on general equilibrium losses, which is important for the informed decision-making process. Last, there are other gaps, including the effect of casualty modeling (fatality and injuries) and other sources of uncertainty of the CGE model and associated economic losses. These other gaps are beyond the scope of this study.

This study aimed to evaluate the impact of multihazard on the community resilience metrics in terms of direct and general equilibrium losses and associated risks from a static perspective. Although the method in this study is generalized for different types of hazards, for an illustrative example, the CSZ and its hazards are considered, namely seismic, tsunami, and joint seismic–tsunami hazards. Although there are several seismic and tsunami hazards, herein seismic ground shaking and tsunami inundation hazards are considered. The effects of liquefaction, landslides, and postearthquake and post-tsunami urban fires are not considered here. The damage and associated losses to buildings are determined at the parcel level using appropriate fragility functions and functionality models available in the literature. The process relies on Monte Carlo simulations (MCSs) to propagate uncertainties in direct damage and loss assessments. Furthermore, the CGE model is used to assess aggregated general equilibrium losses to the community, such as changes in the total employment, domestic supply, and local tax revenue. The methodology is implemented in the open-source Interdependent Networked Community Resilience Modeling Environment (IN-CORE). Seaside, OR, is used as the testbed community with a description of the built environment at the parcel level, full probabilistic hazard analysis for the area, selected fragility functions, functionality and capital stock shock modeling, description of the socioeconomic environment, and economic model. Results are presented in terms of risks associated with direct and general equilibrium losses compared for two hazards across several recurrence intervals. As an important mitigation strategy, these baseline results are then used to evaluate the effectiveness of different seismic retrofit options. Although resilience is generally defined as the ability to withstand, absorb, and recover from a disruptive event, this study does not consider community recovery after the disruption (static resilience). A sensitivity analysis is conducted to understand the effect of building functionality modeling on direct and general equilibrium losses. Finally, discussions and conclusions are presented.

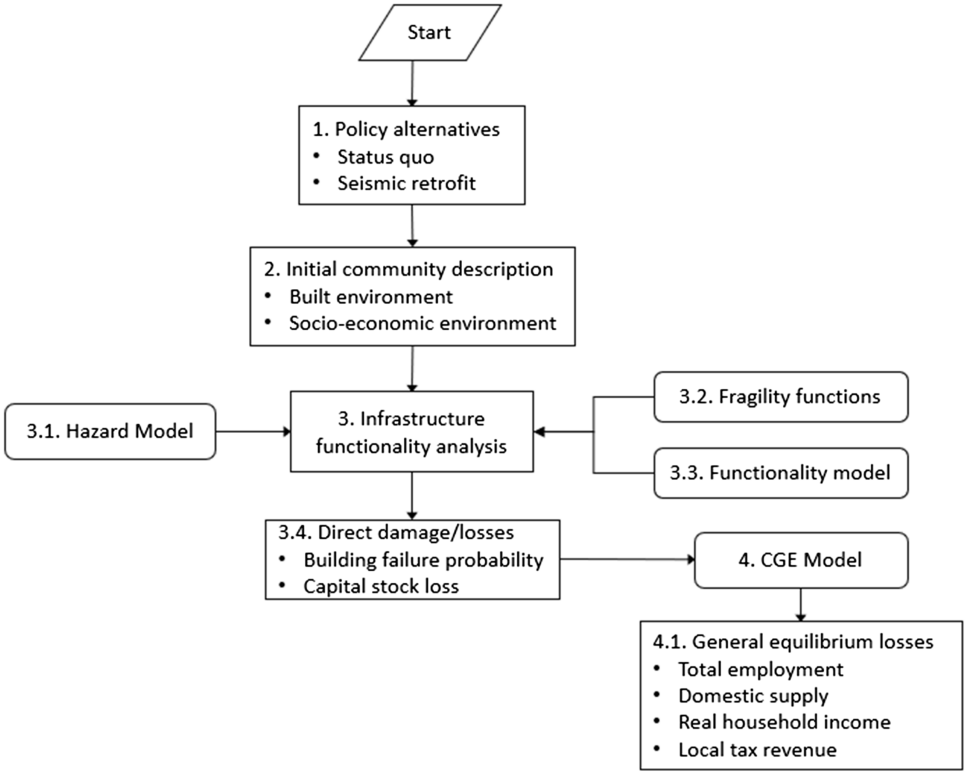

Fig. 1. Proposed methodology for multihazard direct and general equilibrium loss analysis.

Methodology

The methodology (Fig. 1) consists of four main modules: (1) policy alternatives, (2) initial community description, (3) infrastructure functionality analysis, and (4) CGE model. The first module, Policy Alternatives, proposes several decision criteria based on different seismic retrofit options as an important mitigation strategy. The second module, Initial Community Description, consists of essential information about the built environment, such as buildings and associated economic sectors at the parcel level. The third module, Infrastructure Functionality Analysis, comprises four components: hazard model, fragility functions, functionality model, and direct losses. The hazard model consists of the seismic, tsunami, and joint seismic–tsunami hazards for several recurrence intervals. The second component, fragility functions, is used to determine direct damage to buildings. The functionality model is defined based on the level of physical damage to each building. As a result, the failure probability for each building, that is, the probability that a building is not functional, is obtained using a Monte-Carlo simulation with 10,000 iterations. The capital stock loss is calculated for each individual building by multiplying the failure probability by the value of the building. The fourth module includes the CGE model, which describes a set of interactions among households, firms, government, and the rest of the world. Fig. 2 shows the structure of the CGE model as relationships in a circular flow diagram. The households supply labor and capital, receiving wages, profits, and other returns on investments in exchange. They subsequently use this income in conjunction with government transfer payments to consume, save, and pay taxes. Firms produce and sell goods and services using labor and capital purchased from households, as well as intermediate inputs purchased from other firms. Governments tax both households and firms, using the revenue to provide a variety of goods and services. The CGE model considers both supply-side and demand-side changes. Supply-side changes are stimulated by wages, input prices, technology, and taxes, whereas demand-side effects can stem from changes in local household spending, business investment, government expenditure, and regional exports. Founded in microeconomic theory, CGE models evaluate not only direct economic consequences, such as labor force reductions and property

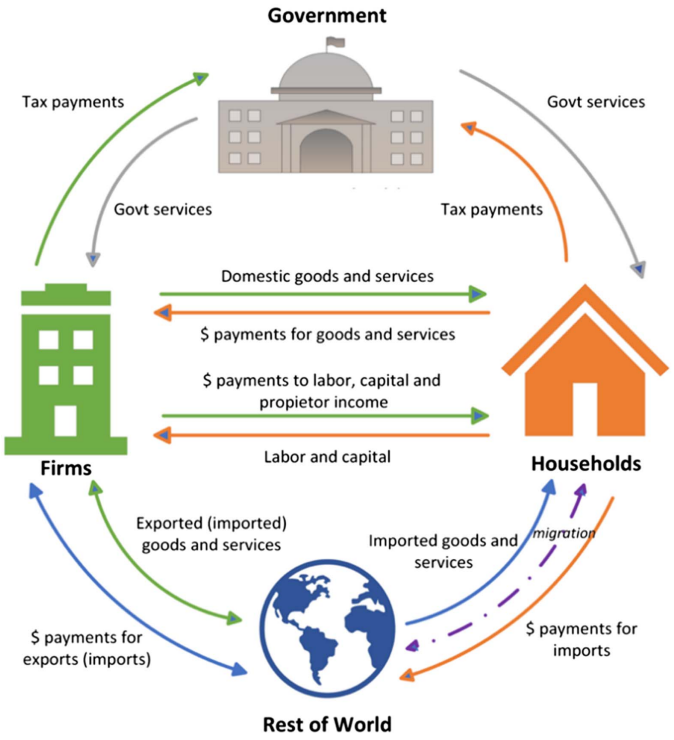

Fig. 2. The computable general equilibrium model structure.

damages, but also associated behavioral responses, leading to total economic impacts, which relate to quantity and price interactions in downstream and upstream markets (Chen et al. 2017). Given the probabilistic hazard model, the economic risk is computed as the expected loss multiplied by the probability of hazard occurrence, which provides insight into events that result in both significant losses and have a high probability of occurrence (Modarres et al. 2016). Due to the selected static perspective, community recovery after the disruption is not considered in this study. More information about each module and their interactions is presented in the following sections.

The methodology developed here is implemented within the Interdependent Networked Community Resilience Modeling Environment. IN-CORE is a robust, open-source computational platform developed by the Center for Risk-Based Community Resilience Planning to integrate engineering and socioeconomic algorithms and model the impact of natural hazards on communities as well as their recovery, evaluate community resilience, and ultimately optimize resilience strategies (Gardoni et al. 2018; van de Lindt et al. 2019, 2023). IN-CORE is freely available online, and a Python library (pyIncore) is available for a variety of researchers from different disciplines.

Multihazard Testbed: Seaside, OR

Seaside is located in Clatsop County, Oregon, in the vicinity of the Cascadia Subduction Zone and vulnerable to both seismic and tsunami hazards (Wood 2007; Goldfinger et al. 2012; OSSPAC 2013). The CSZ is a 1,000-km-long fault stretching from North Vancouver Island to Cape Mendocino in northern California. The CSZ separates the Juan de Fuca and North American plates with varied width along its length. Due to the long length of the fault, the CSZ can cause a megathrust earthquake exceeding magnitude 9.0 (Heaton and Hartzell 1987; Goldfinger et al. 2012). Previous studies showed that Seaside has the highest vulnerability to tsunamis among Oregon coastal communities (Wood 2007; Wood et al. 2010). Although several studies were carried out to assess the physical damage to the infrastructures and direct losses in Seaside due to earthquake and tsunami hazards (e.g., Wiebe and Cox 2014; Park et al. 2017b, 2019; Capozzo et al. 2019; Sanderson et al. 2021b), general equilibrium losses have not been well addressed, particularly for multihazard damage and risk assessments (Chen et al. 2018). The Seaside testbed used in this paper is publicly available (Cox et al. 2022) and consists of four infrastructure systems: buildings, transportation network, electric power network, and water supply network. In this study, only buildings and associated economic sectors were considered to evaluate the direct and general equilibrium losses.

Built Environment

The building characteristics such as construction material, design level, year of construction, and number of stories were identified primarily using tax lot data from Clatsop County (Oregon) with additional spot-checking using Google Street View and a field survey of a limited number of buildings (Park et al. 2017b). For example, Fig. 3 shows the layout of building types and building seismic design levels at the parcel level in Seaside. As shown in Fig. 3(a), a total of 4,679 buildings are identified, all of which are classified as either light frame wood buildings with floor area of less than 5,000 sq. ft. (W1: 2,446 parcels), any wood buildings with floor area greater than 5,000 sq. ft. (W2: 731 parcels), low-rise moment frame buildings (C1L: 1,039 parcels), or midrise concrete moment frame buildings (C1M: 465 parcels). As shown in Fig. 3(b), buildings are also categorized into four different seismic design levels: precode, low-code, moderate-code, and high-code (Park et al. 2017a).

Fig. 3. Layout of buildings at Seaside, Oregon: (a) building types (W1 is light framed wood buildings with a floor area less than 5,000 sq. ft; W2 is commercial, industrial, or multifamily residential wood buildings with a floor area greater than 5,000 sq. ft; C1L is low-rise concrete moment frame buildings; and C1M is mid-rise concrete moment frame buildings); and (b) building design levels. (Base map sources: Esri, DeLorme, HERE, MapmyIndia.)

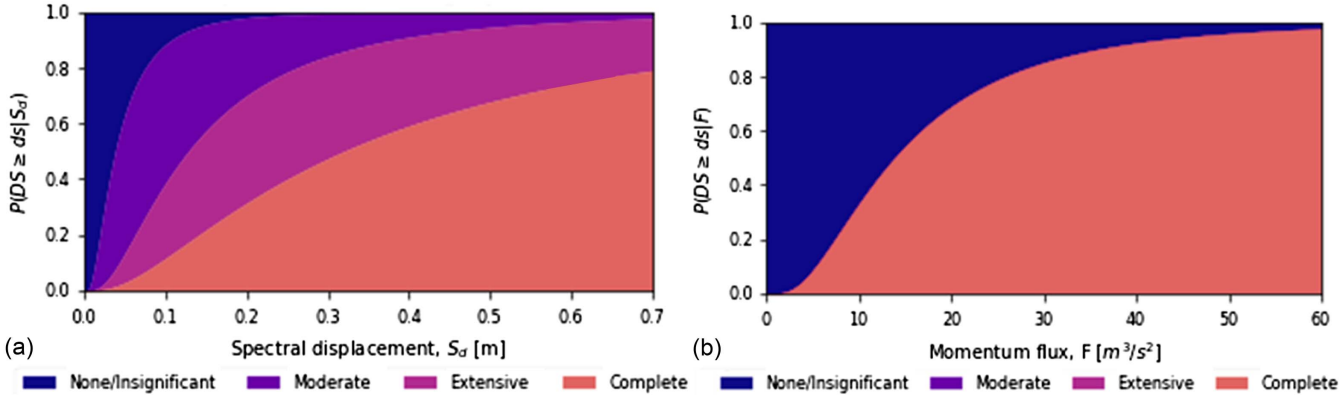

Fig. 4. Examples of fragility functions used in this study for W1 high-code seismic design level: (a) earthquake hazard; and (b) tsunami hazard.

Hazard Model

Probabilistic seismic and tsunami hazards are required to conduct multihazard damage and loss assessments to the built environment. In this study, the results of the Probabilistic Seismic and Tsunami Hazard Analysis (PSTHA) performed in Park et al. (2017a) for Seaside were used. The PSTHA consisted of three main models, the earthquake source model, which included the earthquake fault models and their characteristics; earthquake simulation model, which included the use of ground motion prediction models to simulate the ground shaking intensities; and tsunami model, which included generation, propagation, and inundation modeling. The intensity measures of the earthquake were obtained using the tapered Gutenberg–Richer distribution (Rong et al. 2014) and a ground motion prediction equation (Abrahamson et al. 2016). Given the earthquake source modeling, fault slip distributions were applied to the ComMIT/MOST tool to model tsunami generation and propagation (Titov et al. 2011), whereas COULWAVE was used for the inundation modeling (Lynett et al. 2002). Site-specific annual exceedance probabilities of earthquake and tsunami intensity measures, such as peak ground acceleration (PGA), spectral displacements at various periods of interest, the maximum inundation depth, and the tsunami momentum flux, were computed. This analysis resulted in seismic and tsunami hazard maps associated with seven recurrence intervals, 100, 250, 500, 1,000, 2,500, 5,000, and 10,000 years. However, in this study, focus is placed on the 100-year, 250-year, 500-year, and 1,000-year return periods because larger return period hazards yield such large levels of damage across the community that may render emergency management plans and postdisaster reconstruction and rehabilitation projects unfeasible. In other words, considering such extreme events may not be worthwhile.

Fragility Functions

Direct damage to the built environment due to different hazards can be determined using fragility curves representing the probability of exceeding different damage states for a given hazard intensity. In this study, HAZUS seismic and tsunami lognormal fragility models were used for buildings with associated economic sectors (FEMA 2013, 2015). HAZUS classifies damage states into five categories: none, slight, moderate, extensive, and complete; however, IN-CORE is used for the damage analysis here and is limited to four damage states: none/insignificant (DS_0), moderate (DS_1), extensive (DS_2), and complete (DS_3). In other words, in the fragility curve parametrization developed in IN-CORE, the two damage states None and Slight are combined into one damage state, None/Insignificant. Fig. 4 shows examples of the structural fragility functions for the high-code light-frame wood buildings (W1) used in this work. As shown in Fig. 4, the spectral displacement (S_d) and momentum flux (F) were selected as intensity measures to characterize the seismic and tsunami hazards, respectively. According to the tsunami manual (FEMA 2013), there is no slight damage for the tsunami hazards because it is challenging to distinguish slight damage from no damage. There can, however, be moderate and extensive damage states for some structure types. For W1 (shown in Fig. 4), there are only two possible damage states (none/insignificant and complete). On the other hand, C1M, for example, has moderate, extensive, and complete.

The combined probabilities of damage to the structure due to earthquake and tsunami hazards were calculated based on the HAZUS tsunami manual, assuming that the damage states are statistically independent (Kircher and Bouabid 2014; Park et al. 2019). The combined damage state of buildings ($DS_{EQ\cup Tsu}$) is evaluated based on the Boolean logic rules outlined in the HAZUS Tsunami Manual

$$DS_{EQ\cup Tsu} = \max(DS_{Tsu}, DS_{EQ}) \tag{1}$$

$$DS_{EQ\cup Tsu} = \text{Extensive},\quad \text{if: } \{DS_{Tsu} = \text{moderate and } DS_{EQ} = \text{moderate}\} \tag{2}$$

$$DS_{EQ\cup Tsu} = \text{Complete},\quad \text{if: } \{DS_{Tsu} = \text{extensive and } DS_{EQ} = \text{extensive}\} \tag{3}$$

where DS_{EQ} and DS_{Tsu} = damage states of the building due to earthquake and tsunami only, respectively. Given the functionality model defined in the next section, these probabilities (seismic, tsunami, and joint seismic–tsunami) were sampled from a Monte Carlo simulation consisting of 10,000 iterations to determine the probability of failure for each building.

Functionality and Capital Shock Modeling

To obtain the probability of failure for each building, it is necessary to define the functionality for both residential and commercial buildings. Although recent studies have made efforts to link the functionality model to the full network (e.g., electric and water system), in this study, the functionality model was defined based on building damage states in line with recent publications for other hazards (Roohi et al. 2021; Wang et al. 2022). As mentioned earlier, four damage states, none/insignificant, moderate, extensive, and complete, were considered to determine the direct damage to the

Table 1. Household classification based on income values

Classifications	Income values
Household groups	
HH1	Less than $15,000
HH2	$15,000–$35,000
HH3	$35,000–$75,000
HH4	$75,000–$100,000
HH5	More than $100,000
Labor groups	
L1	Less than $15,000
L2	$15,000–$35,000
L3	$35,000–$75,000
L4	$75,000–$100,000
L5	More than $100,000

buildings. Therefore, two different scenarios were considered: (1) a building is assumed to be nonfunctional if the damage state exceeds DS_0 (that is, the damage state is sampled as DS_1, DS_2, or DS_3), and (2) a building is assumed to be nonfunctional if the damage state exceeds DS_1 (that is, the damage state is sampled as DS_2 and DS_3). Given the fragility function and functionality model, the failure probability of buildings (probability of being nonfunctional) was computed by means of the Monte Carlo simulation through counting a Bernoulli process of functional and nonfunctional samples. Although the failure probability could be obtained directly from damage state probabilities, the Monte Carlo simulation was used to provide the basis for future studies to link the functionality model to the full network. Then, the capital shock losses were computed by multiplying the nonfunctional probabilities by the value of the building. The capital shock losses served as the input for the CGE model to estimate the immediate losses of capital stock and the general equilibrium losses at the community level.

Socioeconomic Environment

According to the 2020 US Census Bureau (2020), the total population of Seaside is estimated at 7,115 people corresponding to 2,898 households. The tourism industry is the mainstay of the economy, and the median household income is $46,505 (in 2019 dollars). Table 1 shows the household and labor classifications based on the income value, which are applied to the CGE model. Wage transfers to households correspondingly, which allows us to evaluate the impact of hazards on income distribution. The losses in capital stock directly impact household income because income sources for each household group consist of labor income, capital returns, and transfers. The decomposition of household and labor allows us to describe how such losses are distributed across income groups. Table 2 shows the different economic sectors and associated capital stock, number of employments, and number of parcels based on the building type. There are 10 main economic sectors—a total of 20 sectors across three zones in Seaside, in which most parcels fall into three categories, housing, service, and retail sectors. Most buildings are in the housing and service sectors, with 2,881 and 450 buildings, respectively.

Fig. 5 shows the layout of the economic environment in Seaside. As shown in Fig. 5(a), the economic sectors are geographically divided into three zones based on Necanicum river and Neawanna creek, Zone 1 (oceanfront), Zone 2 (central), and Zone 3 (inland). For instance, Fig. 5(b) shows the spatial distribution of the housing sector (HS) considering different economic zones. For context, Zone 1 consists mainly of construction, retail, service, health, accommodation, and restaurant sectors; Zone 2 consists of agriculture, construction, manufacturing, retail, service, health, accommodation, and restaurant sectors; and Zone 3 includes agriculture, utilities, construction, retail, service, and health sectors. The capital stock losses can be deaggregated based on these geographical zones, which can provide better insight, particularly for the tsunami hazards because the hazard intensity reduces considerably as one moves away from the shore but varies spatially within the city of Seaside based on proximity to the rivers.

CGE Model

A computable general equilibrium model represents a framework for analyzing the behavioral responses of individuals, businesses, and markets to natural hazard or changes in economic policy, subject to economic account balances and natural resource constraints (e.g., Shoven and Whalley 1992; Dixon and Rimmer 2002; Rose 2004; Rose and Liao 2005; Cutler et al. 2016). The CGE model is based on (1) utility-maximizing households that supply labor (in the local or "rest of world" economy) and capital, using the proceeds to pay for goods and services (both locally produced and imported) and taxes as price-takers in markets; (2) profit-maximizing firms that are perfectly competitive and produce goods and services for both domestic consumption and export by using intermediate inputs, capital stock, land, and labor services; (3) the government sector that collects sales and property taxes used to finance the provision of public services; and (4) the rest of the world, which allows investment flows and trade.

Table 2. Different economic sectors and corresponding information in Seaside

Economic sector	Number of jobs[a]	Capital stock ($M)[b]	Total number of buildings	Number of concrete buildings				Number of wood buildings			
				P-code	L-code	M-code	H-code	P-code	L-code	M-code	H-code
Housing	—	317.30	2,881	7	—	—	—	1,837	564	266	207
Service	907	94.37	450	29	13	9	5	44	341	8	1
Retail	739	61.88	65	20	8	22	2	7	3	3	—
Restaurant	312	52.58	46	25	12	2	5	1	1	—	—
Accommodation	140	23.18	34	8	7	3	1	12	3	—	—
Healthcare	574	41.23	24	9	2	2	—	5	4	2	—
Construction	312	4.72	23	1	—	2	3	7	4	4	2
Manufacturing	602	0.84	7	1	1	1	—	3	—	1	—
Agriculture	71	0.31	2	—	—	—	—	1	—	—	1
Utility	45	0.08	1	—	—	—	—	1	—	—	—

Note: P-code = pre-code; L-code = low-code; M-code = moderate-code; and H-code = high-code.
[a]Quarterly Census of Employment and Wages (QCEW 2017) data.
[b]Clatsop County Assessment and Taxation Data (2017).

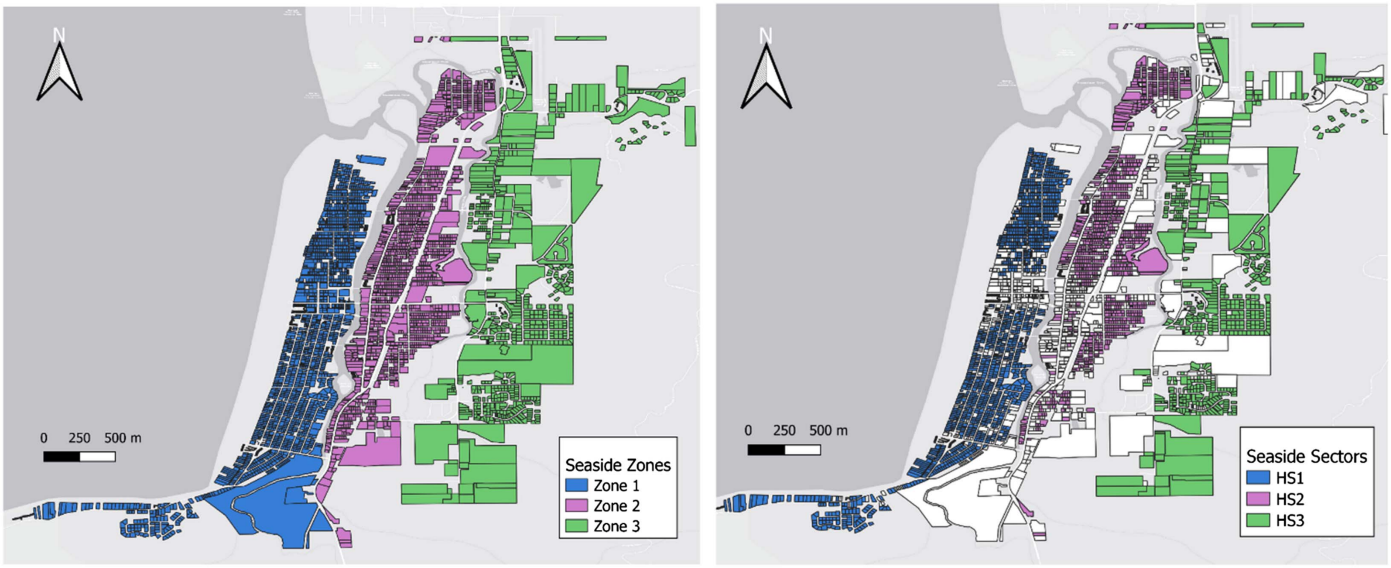

Fig. 5. The layout of economic environment in Seaside: (a) economic zones (Zone 1: oceanfront, Zone 2: central, and Zone 3: inland); and (b) housing economic sectors (HS) located in different zones (HS1 to HS3). (Base map sources: Esri, DeLorme, HERE, MapmyIndia.)

In the CGE model, operationalizing the interactions between actors requires that all transaction flows occurring between these sectors be described in the social accounting matrix (SAM) (Attary et al. 2020). The SAM provides an integrated accounting system that relates production, consumption, the public sector, and investment in a consistent form from both microeconomic and macroeconomic perspectives (Cardenete et al. 2012). To construct a detailed SAM for Seaside, we started with the US Census Bureau's Public Use Microdata Sample (PUMS 2017), which provides sample data with information on the characteristics of each household unit and the people in it, such as distribution of employed workers and wage payments to labor groups assigned to their respective household group. In Seaside, households and workers were distilled into five different wage groups (Table 1). Grouping households and labor this way enabled an investigation of the economic impacts of natural hazards on income distribution. Then we estimated household consumption of that household group by weighting the PUMS data with American Community Survey (ACS) data on consumer expenditure patterns and adjusted by population. In order to identify sectoral employments (Table 2), we used the Quarterly Census of Employment and Wages (QCEW 2017) data, which is a report from Bureau of Labor and Statistics. The QCEW data provided the address of each firm, the number of workers, the total wage bill, and the North American Industrial Classification System (NAICS) code. Workers in the Seaside CGE model were aggregated into 20 sectors across three zones based on the NAICS employment categories.

We next established the aggregated sectors' demand for capital and land in the production sectors. Capital stock values were collected from the Clatsop County Assessor's data, which indicates the use of each parcel of land in the county, including the address, acreage, assessed value, and the value of any structures. These properties were assigned to Seaside spatially using latitude and longitude coordinates. Households demand housing services from these properties; thus, we identified residential properties to derive housing sectors in three zones, HS1, HS2, and HS3. To organize commercial properties, we augmented the County Assessor's data with the QCEW data. We matched the QCEW data with the Assessor's data to obtain data for firms in Seaside, with data for land used, assessed value of the building, value of the structure, and associated NAICS code. These data were aggregated into the 20 commercial sectors across three zones in Seaside.

The City of Seaside organizes government revenue and expenditure data in a document that is referred to as the Comprehensive Annual Financial Report (CAFR 2017). We used Seaside's CAFR to identify sales, property, and other taxes collected from firms, households, and tourists. In addition, the CAFR reports city expenditures on public services such as police, fire, and administrative services, which represent the local government expenditure in the SAM. We also used Bureau of Economic Analysis data to estimate input–output coefficients of intermediate inputs and the relationship between capital and investment. The allocation of resources is determined by changes in relative prices for goods, services, labor, capital, and land. In summary, we constructed a spatial SAM and CGE model that allowed for modeling of the disparate impacts of the natural hazards on the Seaside economy. We confirmed that the destructive nature of the earthquake and tsunami had uneven impacts on the capital stock across the 20 commercial sectors as well as the three housing sectors.

Results

This section presents the results of analyses in terms of direct and general equilibrium losses. The direct damage and loss consist of building failure probabilities and capital stock losses at the parcel and community levels, respectively. Scenario 2, mentioned earlier, is selected as the functionality model in this section (i.e., a building is nonfunctional if the damage state exceeds DS_1). The capital stock losses were deaggregated by the hazard and the economic zone to provide a better understanding of the impact of the hazards to the economic system. As mentioned earlier, capital stock losses were supplied as an input to the CGE model. As a result, general equilibrium losses were estimated in terms of changes in the total

Fig. 6. Probability of parcel failure (i.e., probability of being nonfunctional) for the 500-year recurrence interval: (a) seismic; (b) tsunami; and (c) joint seismic–tsunami. (Base map sources: Esri, DeLorme, HERE, MapmyIndia.)

employment, domestic supply, real household income, and taxes (sales, property, and accommodation taxes). As mentioned earlier, the economic risk is calculated as the expected loss multiplied by the probability of hazard occurrence (inverse of the recurrence interval), which provides an understanding of both significant loss and a high probability of occurrence. The CGE results provide long-run equilibrium with no external injections, such as recovery assistance. In other words, these results describe how the economy would look in the long term if there were no government expenditure for repair or reconstruction. For the 100-year recurrence interval, direct and general equilibrium losses are not presented because the resulting impacts were insignificant. Therefore, the results for 250-year, 500-year, and 1,000-year recurrence intervals are discussed. Finally, sensitivity analysis was conducted to investigate the effect of building functionality models on both direct and general equilibrium losses.

Direct Losses and Risks

Fig. 6 shows the probability of building failure at the parcel level for the 500-year recurrence interval considering different hazards: seismic, tsunami, and joint seismic–tsunami. The probabilities of failure, defined as the probability of the parcel being nonfunctional, were obtained from Monte Carlo simulation consisting of 10,000 realizations. As shown in Fig. 6(a), the probability of failure for the seismic hazard was quite uniform, with a maximum observed at 57%. This uniformity is somewhat expected because the seismic intensity mostly depends on the source-to-site distance and soil type, neither of which vary much across the region (Park et al. 2017a). In contrast to the seismic hazard, as shown in Fig. 6(b), only buildings located on the oceanside experienced a high probability of being nonfunctional due to the tsunami hazard. The dark red means a 100% probability of being nonfunctional, and dark green means a 100% probability of being functional. The probability of failure resulting from joint seismic–tsunami hazards is shown in Fig. 6(c). As was expected, the joint probability of failure increased only for buildings located on the oceanside of the region.

Table 3 indicates the capital stock losses for different economic sectors due to different hazards and three recurrence intervals, 250, 500, and 1,000 years. Regarding seismic hazards, capital stock losses were significant for all economic sectors. For example, regardless of the recurrence interval, two economic sectors, ACCOM and HC, had the highest capital stock losses (bold underlined values). The maximum capital stock loss was observed in the accommodation sector as 48.15% occurring due to the 1,000-year earthquake recurrence interval. Concerning tsunami hazard, all capital stock losses were negligible for two recurrence intervals, 250 and 500 years, due to the low level of inundation occurring in all economic zones. However, by increasing the tsunami recurrence interval to 1,000 years, the housing sector, which is the most significant sector, with 2,881 buildings in Seaside, experienced the highest capital stock loss of 52.13%. Concerning joint seismic–tsunami hazards, the ACCOM and HC sectors had the highest capital stock losses compared to other sectors.

Fig. 7 allows for a comparison of capital stock losses and related risks for the HS sector aggregated by the economic zone. As shown in Fig. 7(a), the highest capital stock losses were observed, at about 24%, 52%, and 63%, associated with 1,000-year seismic, tsunami, and joint seismic–tsunami recurrence intervals, respectively. Conversely, as shown in Fig. 7(b), the highest economic risk occurred for the 500-year and 1,000-year joint seismic–tsunami. In addition, as the recurrence interval increased, capital stock losses due to the tsunami hazard began to be underlined, particularly for the 1,000-year tsunami hazard.

Fig. 8 compares the SERV sector's capital stock losses and associated economic risks. The results indicate that the SERV sector experienced lower capital stock losses than the HS sector due to the tsunami hazard. Therefore, the economic risks were significantly lower, and its maximum value occurred for the 250-year joint seismic–tsunami. With regard to the tsunami hazard, the capital

Table 3. Percentage of capital stock losses for different economic sectors and recurrence intervals for earthquake, tsunami, and earthquake and tsunami hazards

	Earthquake			Tsunami			Earthquake + tsunami		
Sectors	250-year	500-year	1,000-year	250-year	500-year	1,000-year	250-year	500-year	1,000-year
HS	11.00	18.77	23.76	**0.80**	**16.42**	**52.13**	11.74	31.86	63.19
SERV	15.58	27.90	33.74	0.01	0.97	11.91	15.88	28.46	44.77
REST	18.65	33.53	41.69	0.00	0.36	23.39	18.89	34.27	56.70
RETAIL	13.16	25.17	31.74	0.00	0.70	6.10	13.52	25.69	36.79
ACCOM	10.52	**36.70**	**48.15**	0.01	0.81	20.57	10.83	**38.35**	**65.90**
HC	**19.56**	32.62	39.33	0.00	0.09	1.37	**19.63**	32.86	41.95
UTIL	16.50	25.30	32.40	0.00	0.50	4.40	17.30	26.50	35.90
CONST	8.62	17.27	22.97	0.01	0.42	7.10	8.83	17.42	28.03
MANUF	14.94	25.88	31.48	0.00	0.02	17.47	15.25	25.97	43.13
AG	12.63	18.95	28.60	0.00	0.26	3.58	12.93	20.44	29.44

Note: HS = housing sector; SERV = service sector; REST = restaurant sector; RETAIL = retail sector; ACCOM = accommodation sector; HC = health sector; UTIL = utility sector; CONST = construction sector; MANUF = manufacturing sector; and AG = agriculture sector. The bold values correspond to the highest capital stock loss for each recurrence interval.

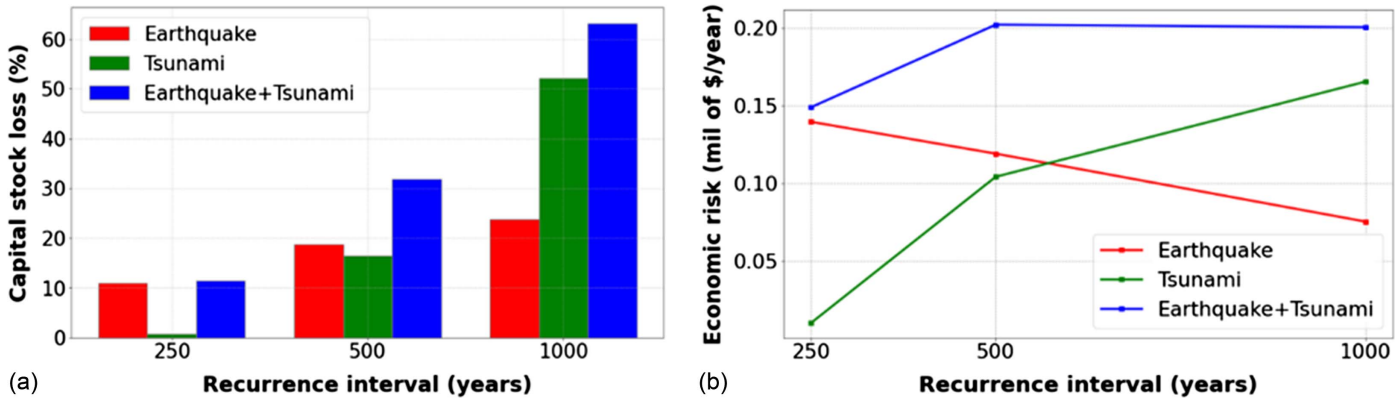

Fig. 7. Capital stock loss for housing sector (HS): (a) percentage loss; and (b) economic risk.

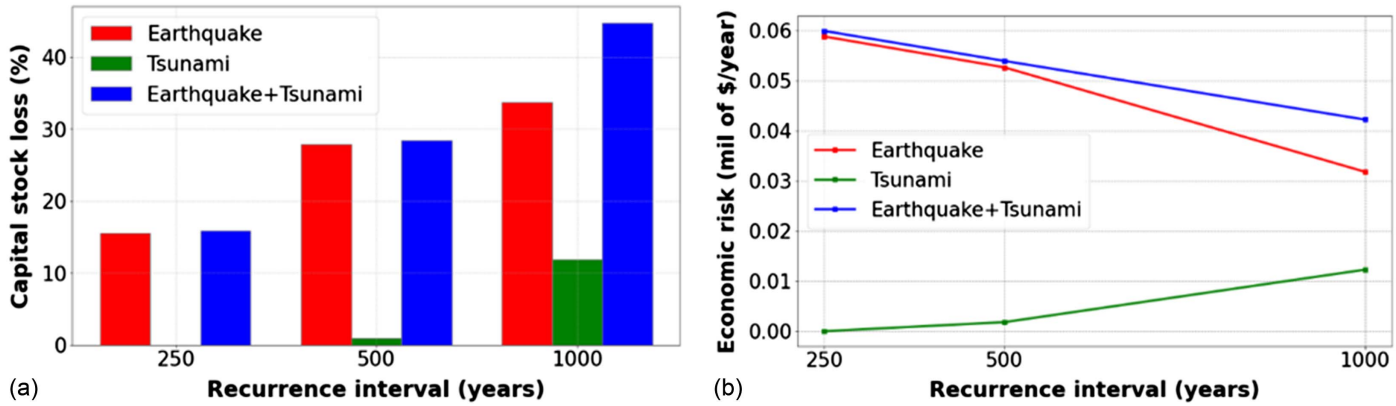

Fig. 8. Capital stock loss for service sector (SERV): (a) percentage loss; and (b) economic risk.

stock losses for the SERV sector were negligible. Results indicate a low level of damage because most buildings associated with the SERV sector are located in Zones 2 and 3, that is, the central and inland zones, where the tsunami intensity is not significant even for the 1,000-year recurrence interval. Correspondingly, as shown in Fig. 8(b), the risks associated with the tsunami hazard were almost zero for 250-year and 500-year recurrence intervals for the SERV sector.

Capital stock losses can be compared among different economic sectors deaggregated by hazards and economic zones. A detailed example (Table 8) and corresponding descriptions are provided in Appendix. The results show that capital losses were dependent on the building type, hazard type, and economic zones. For example, capital stock losses of the HS sector for the seismic hazard were almost identical across different economic zones (Zones 1, 2, and 3). However, for the tsunami hazard, the maximum value of

Table 4. Example of CGE results for hazards with the 500-year recurrence interval

Resilience metrics	Category	Earthquake 500-year Amount of loss	Earthquake 500-year Percentage loss	Tsunami 500-year Amount of loss	Tsunami 500-year Percentage loss	Earthquake + tsunami 500-year Amount of loss	Earthquake + tsunami 500-year Percentage loss
Total employment (person)	—	248	6.3	57	1.4	299	7.5
Domestic supply ($M)	—	204.27	13.9	31.68	2.2	232.7	15.8
Real household income[a] ($M)	HH1	0.04	1.7	0.03	1.4	0.08	3.3
	HH2	1.01	3.7	0.00	0.0	1.05	3.8
	HH3	5.62	4.3	0.58	0.4	6.31	4.8
	HH4	3.89	4.8	0.55	0.7	4.46	5.5
	HH5	15.38	5.4	2.98	1.1	17.99	6.3
	Total	25.94	4.9	4.08	0.8	29.81	5.7
Local tax revenue ($M)	STPIT	0.72	5.1	0.12	0.9	0.84	5.9
	Sales	0.07	5.0	0.01	0.8	0.08	5.8
	Property	0.11	3.2	0.02	0.6	0.13	3.7
	Accommodation	0.05	6.6	0.02	2.7	0.06	9.3
	CYGF	2.10	32.3	0.31	4.9	2.31	37.1
	Total	2.96	11.4	0.48	1.8	3.42	13.1

Note: STPIT = state personal income tax; and CYGF = city general fund.
[a]The real household income is presented based on the different household groups (Table 1).

capital stock loss occurred in the oceanfront zone (Zone 1). A similar comparison can be given for other economic sectors that are not presented here for brevity. These outputs can offer a better understanding of potential direct losses to different economic sectors, which can help to identify and prioritize the vulnerable economic sectors in the community.

General Equilibrium Losses and Risks

Table 4 shows an example of CGE results for different hazards for the 500-year recurrence interval. For example, the total employment was reduced by about 6.3%, 1.4%, and 7.5% due to the seismic, tsunami, and joint seismic–tsunami hazards, respectively. The domestic supply experienced losses of 13.9%, 2.2%, and 15.8% for different hazards, respectively. Regarding the real household income, for the seismic hazard, increasing the household classification from HH1 to HH5 resulted in higher losses in income because households with higher incomes typically own higher percentages of the physical capital, which is likely to experience damage and a subsequent reduction in capital returns. Given the tsunami hazard, HH1 households were mostly impacted because economic sectors, such as SERV1, REST1, and RETAIL1, located in the oceanfront zone (Zone 1) significantly contributed to the corresponding labor income. For joint seismic–tsunami hazards, HH5 households experienced a maximum income loss of $17.9 million or 6.3%. Total losses for real household income due to seismic, tsunami, and joint seismic–tsunami hazards were about 4.9%, 0.8%, and 5.7%, respectively. Finally, the city general fund sustained the maximum reduction, in which losses for seismic and tsunami hazards were $2.1 million (32.3%) and $0.31 million (4.9%), respectively. For the tsunami hazard, whereas the city general fund experienced the highest loss, the reduction in accommodation tax was higher than other tax-related losses, such as sales and property taxes, because hotels and recreational properties are frequently located near the coast, where they are more vulnerable to the tsunami hazard. Total losses for the local tax revenue due to seismic, tsunami, and joint seismic–tsunami hazards were about 11.4%, 1.8%, and 13.1%, respectively. Similar results can be obtained for other recurrence intervals, in which losses for the 100-year recurrence interval were more considerable. Similarly, the CGE results can be compared

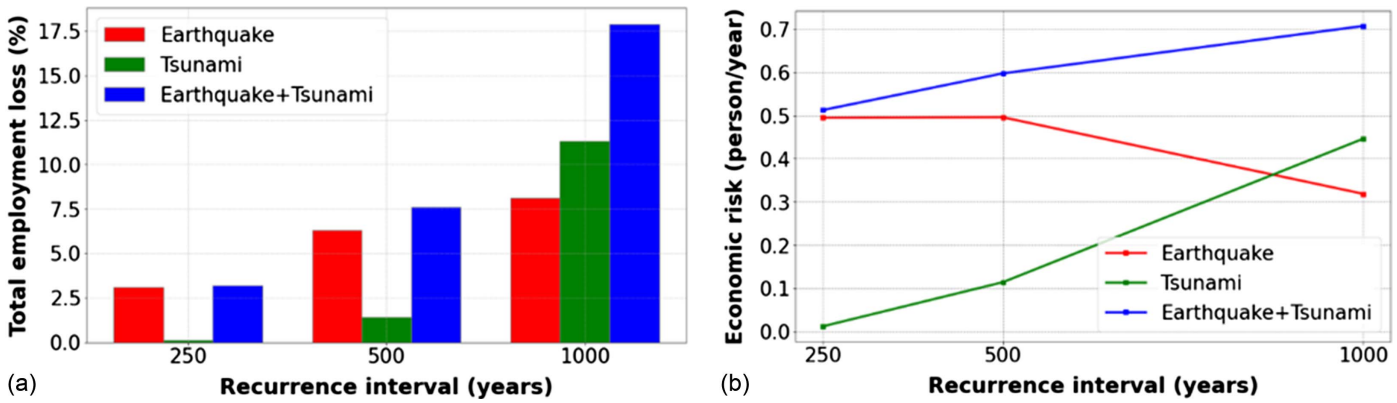

Fig. 9. Total employment loss for different hazards: (a) percentage loss; and (b) economic risk.

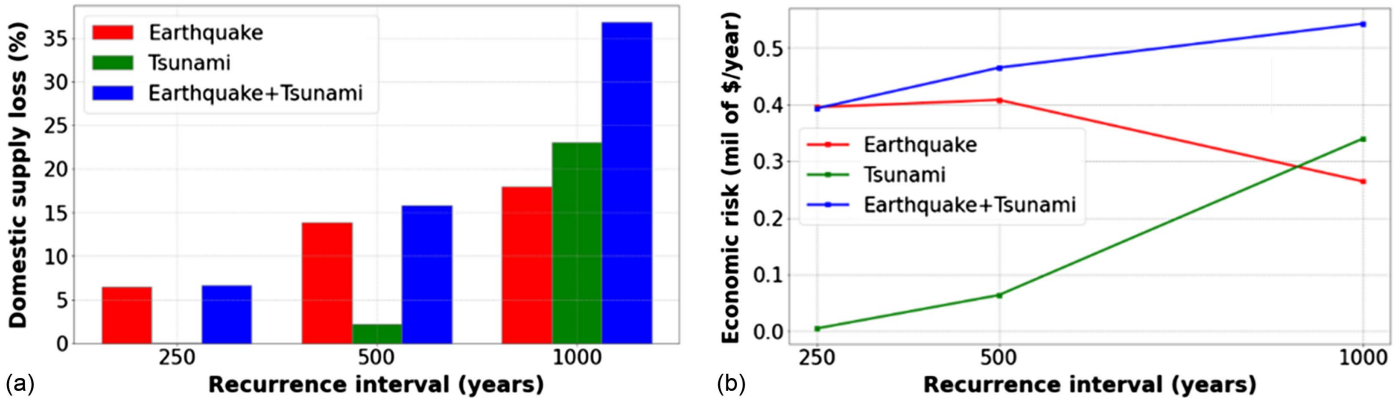

Fig. 10. Domestic supply loss for different hazards: (a) percentage loss; and (b) economic risk.

across different economic zones. Table 9 in Appendix illustrates the spatially deaggregated CGE results, including losses in total employment and domestic supply.

Fig. 9 shows the effect of different hazards on the total employment loss in terms of percentage and associated risks. By increasing the recurrence interval, the total employment loss increased, in which its maximum belonged to the 1,000-year joint seismic–tsunami hazards. Similarly, the highest risk was associated with 1,000-year joint seismic–tsunami hazards. As shown in Fig. 9(b), for the tsunami hazard, the risks were insignificant for 250 and 500 years compared to the seismic hazard. Fig. 10 shows a similar type of results for the domestic supply change. As shown in Fig. 10(b), for the seismic hazard, increasing the recurrence interval from 250 to 1,000 years led to a considerable increase in the economic risk (almost by a factor of 1.5). Regarding the tsunami hazard, the economic risk remained almost zero for the 250-year recurrence interval and then slightly increased by varying the recurrence interval.

Fig. 11 compares the effect of different hazards on the household income loss and associated risk deaggregated by the income classification. Regardless of the income classification, the maximum reduction in the household income of the HH5 occurred due to joint seismic–tsunami hazards. For the tsunami hazard, the income loss was negligible for the 250-year and 500-year recurrence intervals, and it significantly increased for the 1,000-year recurrence interval. For example, for 1,000-year joint seismic–tsunami hazards, the HH5 experienced about a 16% reduction in income ($45.7 million), resulting in the highest economic risk of $0.045 million per year. Regarding the seismic hazard, although income losses were identical by varying recurrence intervals, the annualized risk decreased for the 1,000-year recurrence interval.

Retrofitting Analysis

The methodology was applied to evaluate how different seismic retrofit strategies can reduce direct and general equilibrium losses and associated risks. We assumed three seismic retrofit strategies: (1) design level of only residential buildings increased to the high code, (2) design level of only commercial buildings increased to the high code, and (3) design level of all buildings increased to the high code. The comparisons for different hazards and recurrence intervals are presented. The cost of the seismic retrofit strategy and its impact on the decision-making process were not considered for this analysis.

Tables 5–7 show the results of different seismic retrofit strategies for 500-year recurrence intervals. The results indicate that retrofitting only residential buildings (Retrofit 1) did not considerably reduce direct and general equilibrium losses. For example, for the seismic hazard (Table 5), the average capital stock loss was slightly reduced from 23.8% to 21%. Similar results were also observed for general equilibrium losses. However, the decrease was more notable for the tsunami hazard (Table 6) because the retrofit of wood-frame buildings seems to be more effective against the tsunami hazard compared to the seismic hazard. For the second retrofit strategy (Retrofit 2), as expected, retrofitting only commercial buildings resulted in a significant decrease in losses, particularly general equilibrium losses. For example, for the seismic hazard, the total employment loss was reduced by about 44%, from 247

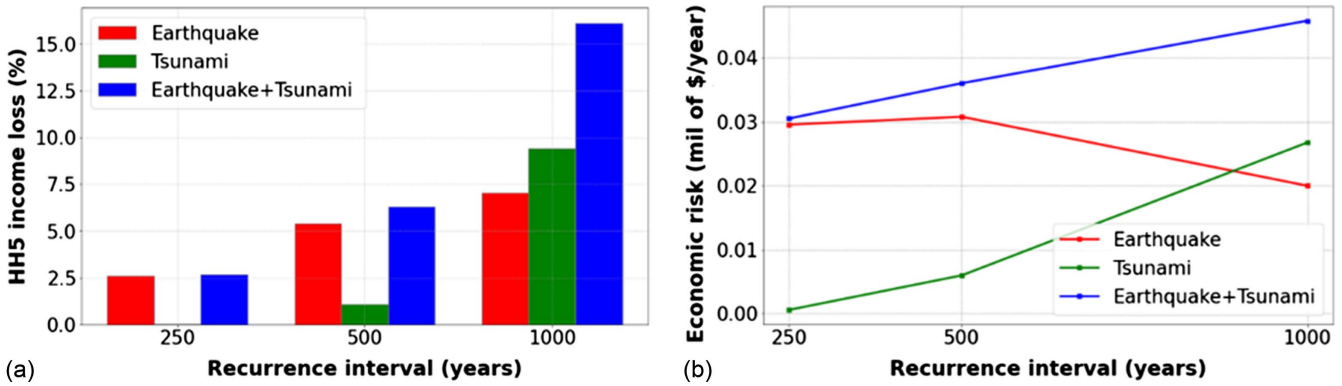

Fig. 11. The HH5 income loss for different hazards: (a) percentage loss; and (b) economic risk.

Table 5. Results of the seismic retrofit for the 500-year recurrence interval seismic hazard

Resilience metrics	Category	Earthquake			
		500-year Status quo	500-year Retrofit 1	500-year Retrofit 2	500-year Retrofit 3
Average capital stock loss (%)	—	23.8	21	13.8	10.6
Total employment (person)	—	247 (6.4%)	220 (5.5%)	139 (3.5%)	110 (2.8%)
Domestic supply ($M)	—	203.79 (13.8%)	188.86 (12.8%)	108.09 (7.3%)	93.05 (6.3%)
Real household income ($M)	Total	25.83 (4.9%)	23.84 (4.5%)	13.54 (2.6%)	11.42 (2.17%)
Local tax revenue ($M)	Total	2.94 (11.3%)	2.73 (10.5%)	1.52 (5.8%)	1.29 (4.9%)

Table 6. Results of the seismic retrofit for the 500-year recurrence interval tsunami hazard

Resilience metrics	Category	Tsunami			
		500-year Status quo	500-year Retrofit 1	500-year Retrofit 2	500-year Retrofit 3
Average capital stock loss (%)	—	4.4	2.6	1.1	1.1
Total employment (person)	—	58 (1.5%)	32 (0.8%)	42 (1.1%)	16 (0.4%)
Domestic supply ($M)	—	33.28 (2.3%)	22.71 (1.5%)	17.67 (1.2%)	7.31 (0.5%)
Real household income ($M)	Total	4.21 (0.8%)	2.74 (0.5%)	2.52 (0.5%)	1.06 (0.2%)
Local tax revenue ($M)	Total	0.5 (1.9%)	0.34 (1.3%)	0.27 (1.1%)	0.12 (0.5%)

Table 7. Results of the seismic retrofit for the 500-year recurrence interval joint seismic–tsunami hazards

Resilience metrics	Category	Earthquake + tsunami			
		500-year Status quo	500-year Retrofit 1	500-year Retrofit 2	500-year Retrofit 3
Average capital stock loss (%)	—	27.3	22.4	16.7	11.7
Total employment (person)	—	299 (7.6%)	242 (6.1%)	183 (4.6%)	127 (3.2%)
Domestic supply ($M)	—	232.38 (15.8%)	205.16 (13.9%)	127.52 (8.7%)	100.86 (6.8%)
Real household income ($M)	Total	29.79 (5.7%)	25.84 (4.9%)	16.45 (3.1%)	12.61 (2.4%)
Local tax revenue ($M)	Total	3.42 (13.1%)	2.97 (11.4%)	1.86 (7.1%)	1.42 (5.4%)

Fig. 12. Comparison of status quo and retrofit cases (Retrofit 2: design level of only commercial buildings increases to the high code; Retrofit 3: design level of all buildings increases to the high code) for the 500-year recurrence interval seismic hazard.

to 139 persons. In addition, the loss in the local tax revenue was reduced by about 48%, from $2.9 to $1.52 million. The same levels of reductions in tax losses were observed for tsunami and joint seismic–tsunami hazards. Finally, although retrofitting all buildings (Retrofit 3) resulted in the lowest losses, given the high expected retrofit cost, it may not be the most efficient option for the community. Fig. 12 compares the results of Retrofits 2 and 3 for the seismic hazard associated with the 500-year recurrence interval. The comparison shows that retrofitting only commercial buildings could reduce losses, particularly general equilibrium losses such as local tax, as much as retrofitting all buildings in the community.

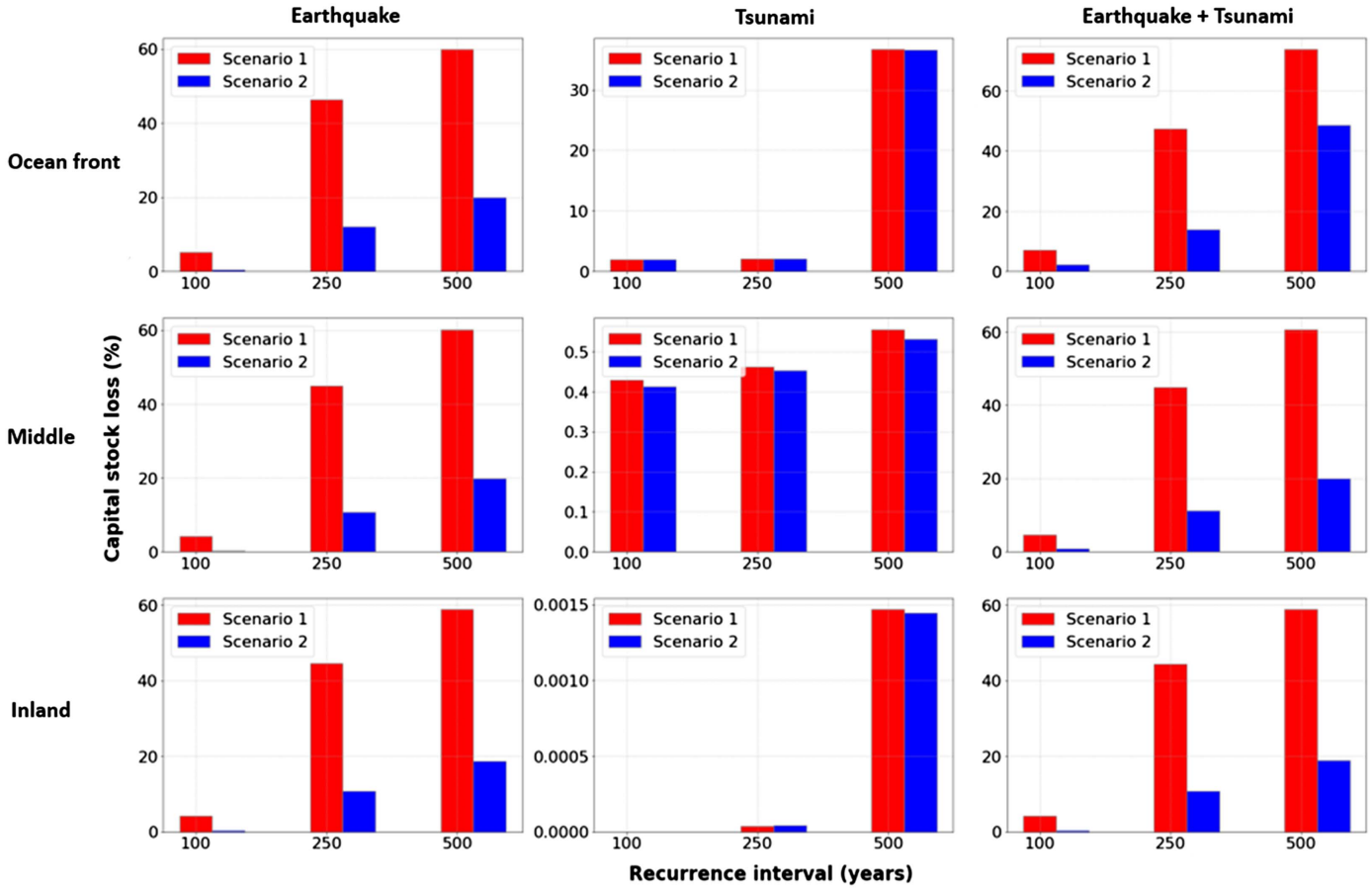

Fig. 13. The effect of the building functionality model on capital stock losses to the housing sector (HS) located in different zones.

Sensitivity Analysis

This section incorporates a sensitivity analysis to assess how different definitions of building functionality affect direct and general equilibrium losses. As mentioned earlier, two different scenarios were considered to define the functionality of buildings, Scenario 1, where a building is nonfunctional if the damage state exceeds DS_0, and Scenario 2, where a building is nonfunctional if the damage state exceeds DS_1. Fig. 13 shows the effect of building functionality on capital stock losses to the housing sector deaggregated by the hazard type (columns) and economic zone (rows). The results were compared for 100-year, 250-year, and 500-year recurrence intervals. Regardless of the economic zone, for the seismic hazard, using different functionality models significantly affected capital stock losses. For instance, considering the 500-year recurrence interval for the seismic hazard, the capital stock loss decreased from 60% to 20% by varying the functionality model from Scenario 1 to 2. Similar results were observed for joint seismic–tsunami hazards. However, the capital stock loss was independent of the functionality model for the tsunami hazard because the tsunami fragility functions adopted for IN-CORE [see Fig. 4(b)] had fewer damage states than seismic fragility functions, particularly for low-rise and light-frame buildings, and therefore were not sensitive to the functionality definitions for Scenarios 1 and 2.

As another example, Fig. 14 shows the effect of the building functionality modeling on the domestic supply loss and associated risks due to different hazards. The maximum domestic supply loss and associated risk values occurred when Scenario 1 was selected as the building functionality model. Furthermore, for the seismic hazard and Scenario 1, although the maximum domestic supply loss occurred for the 1,000-year recurrence interval, the highest risk belonged to the 500-year recurrence interval. A similar trend was observed for joint seismic–tsunami hazards. However, for the tsunami hazard, the results were less sensitive to the functionality modeling, which was expected considering the tsunami fragility functions and their limited number of damage states used in this study.

Discussion

This paper proposes a methodology to evaluate the impact of multiple joint hazards on the economic resilience metrics, that is, direct losses such as capital stock loss and general equilibrium losses such as number of workers, domestic losses, and local tax revenue. The methodology consisted of several modules: policy alternatives, initial community description, infrastructure functionality analysis, and CGE modeling. The city of Seaside, Oregon, was selected as the testbed community. The methodology was applied to quantify the effect of different seismic retrofit options as an important mitigation strategy on the resilience metrics. This section presents a discussion and outlines some insights gained from results presented in previous sections.

Results indicate that the vulnerability of economic sectors depended on the building and hazard types and that it varied with the recurrence interval. For example, economic sectors located in Zone 1 (ocean front) were more vulnerable to the tsunami hazard compared to Zone 2 (central) and Zone 3 (inland). Furthermore, economic risks were sensitive to the hazard type, in that the maximum values were associated with 500-year and 1,000-year recurrence intervals for seismic and tsunami hazards, respectively. Similar

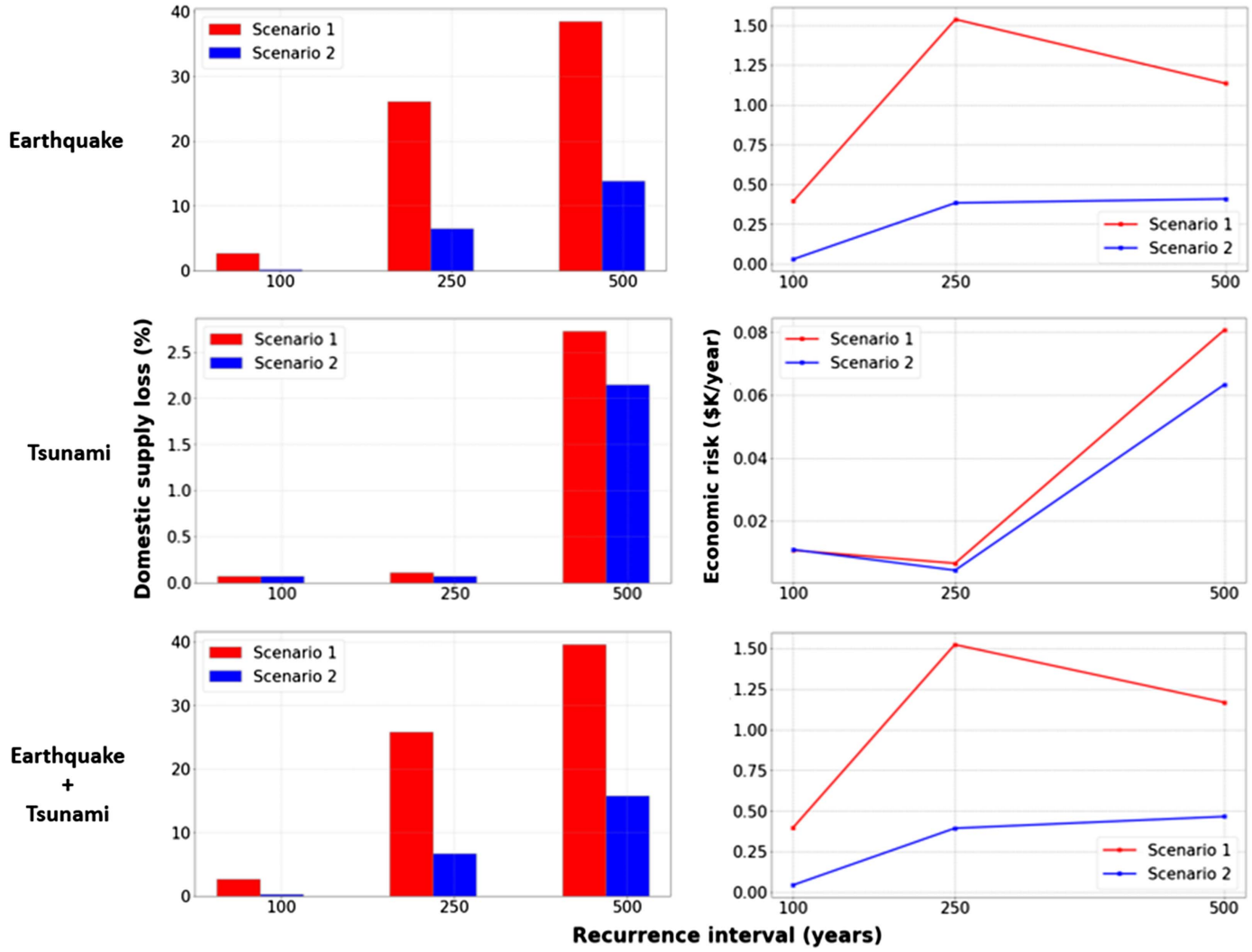

Fig. 14. Effect of building functionality modeling on the domestic supply loss and associated risks.

outcomes were observed for general equilibrium losses. For the seismic hazard, increasing the household classification from HH1 to HH5 resulted in higher losses in upper income groups; however, for the tsunami hazard, HH1 households were mostly impacted because the economic sectors located in Zone 1 significantly contribute to the corresponding labor income. Regarding the tax losses, the city general fund experienced the maximum reduction. Given the 500-year recurrence interval, the local tax revenue was reduced by about 11.4%, 1.8%, and 13.1% for seismic, tsunami, and joint seismic–tsunami hazards, respectively. The losses were significantly decreased by applying different seismic retrofit strategies (Tables 5–7). The comparisons show that retrofitting only commercial buildings to the high code is an efficient strategy to reduce both direct and general equilibrium losses. The sensitivity analysis indicated that different definitions of building functionality result in distinct outcomes (Figs. 13 and 14). For example, given the 500-year recurrence interval of the seismic hazard, the capital stock loss decreased from 60% to 20% by varying the functionality model.

As potential highlights for future research, first, the CGE model needs to be improved to include extreme events with a higher recurrence interval in the analysis. Extreme events are likely to destroy a large portion of the capital stock in the city, and the existing CGE model cannot predict general equilibrium losses accurately when capital stock shocks are too large. Given larger shocks, because the economy has limited substitutes between intermediate inputs, the model cannot be converged to the optimal solution. Second, the functionality model for buildings needs to be extended to account for infrastructure systems, such as water and power networks and their independencies (e.g., Wang et al. 2022). For example, a building can experience a low level of damage, but it is only partially functional or nonfunctional without electricity, unless the parcel has a generator. Third, a cost-benefit analysis needs to be implemented for different seismic retrofit strategies in order to provide better insight for emergency planners and decision makers (Wang et al. 2021). Last, the CGE model needs to be improved to include changes in labor supply due to fatalities, injuries, and outmigration. For example, results in Amini et al. (2022) indicated that seismic retrofitting of buildings significantly reduces casualties, which will also impact labor supply and the CGE model. Thus, subsequent general equilibrium losses and reduction of the tax base should be explored with improved CGE models.

Conclusion

This paper proposed a methodology to evaluate the impact of multihazard on the economic resilience metrics in terms of direct damage

and losses such as the building failure probability and the capital stock loss and general equilibrium losses such as the number of employments and domestic supply. The city of Seaside, Oregon, vulnerable to both earthquake and tsunami due to its proximity to the CSZ, was selected as a case study to illustrate the application of the methodology. Although there are several seismic and tsunami hazards, herein only seismic ground shaking and tsunami inundation hazards were considered. The direct damage and losses to buildings and economic sectors were obtained at the parcel and community level using appropriate fragility functions and functionality models. The process relied on Monte Carlo simulations to propagate uncertainties in damage, functionality, and loss models. Given the direct losses, the CGE model was used to assess aggregated general equilibrium losses to the community. The economic risks were also determined based on the probabilistic hazard. The methodology was used to quantify how different seismic retrofit options can affect the resilience metrics. Finally, a sensitivity analysis was conducted to evaluate how different definitions of building functionality affect the outcomes. The main conclusion from this work are:

1. Results indicate that the vulnerability of economic sectors depends on the hazard type, economic zone, and building type and varies with the recurrence interval. For example, the accommodation and housing sectors were the most vulnerable to seismic-only and tsunami-only hazards. In addition, the housing sector located in Zone 1 at the ocean front (HS1) was more vulnerable than HS2 and HS3 located in other zones. Comparable results were also observed for risks, in which the highest risks were associated with the 500-year event for the seismic recurrence interval and the 1,000-year for tsunami and joint seismic–tsunami hazards, respectively.
2. The results of the CGE model show that general equilibrium losses depended on the hazard type, hazard severity, and economic zones. For example, the total employment was reduced by 6.3%, 1.4%, and 7.5% due to the seismic, tsunami, and joint seismic–tsunami hazards, respectively. Regarding the real household income, HH5 and HH1 households suffered the maximum income losses for seismic and tsunami hazards, respectively. Similar trends were observed for tax-related losses. For instance, whereas the city general fund experienced the highest losses, for the tsunami hazard, the reduction in accommodation tax was higher than other tax losses because hotels and recreational properties are frequently located near the coast (Zone 1) and thus are more susceptible to the tsunami hazard. Regarding the economic risk, for the tsunami hazard, the risks were insignificant for the 250-year and 500-year recurrence intervals compared to the seismic hazard. Finally, the maximum risk belonged to the 1,000-year joint seismic–tsunami hazards.
3. Direct and general equilibrium losses and associated risks were significantly reduced by using seismic retrofit strategies. Results show that retrofitting only residential buildings had a large impact on reducing general equilibrium losses. Comparisons show that although retrofitting all buildings to the high code (Retrofit 3) resulted in the lowest losses, given the high expected retrofit cost, retrofitting only commercial buildings (Retrofit 2) may be an efficient retrofit option for the community. For example, given the 500-year joint seismic–tsunami hazards, the domestic supply was reduced from 15.8% to 8.7% and 6.8% for Retrofits 2 and 3, respectively.
4. The results of the sensitivity analysis show that losses and associated risks are sensitive to the definition of building functionality, particularly for the seismic hazard. For example, given the seismic hazard, the highest domestic supply risk associated with the 250-year recurrence interval decreased from \$1.5 to \$0.4 million/year for Scenarios 1 and 2, respectively. Similar results were observed for joint seismic–tsunami hazards. This high level of sensitivity highlights the necessity for a common

Table 8. Percentage of capital stock losses for different economic sectors deaggregated by associated economic zones

	Earthquake			Tsunami			Earthquake + tsunami		
Sectors	250-year	500-year	1,000-year	250-year	500-year	1,000-year	250-year	500-year	1,000-year
HS1	11.98	19.93	24.84	2.09	**36.68**	90.89	13.84	**48.67**	92.7
HS2	10.98	19.72	24.78	0.44	0.54	32.39	11.26	20.2	49.04
HS3	10.79	18.64	24.69	0	0	0.01	10.81	18.76	24.75
SERV1	12.47	24.96	31.74	0.02	8.06	64.35	12.41	31.51	79.43
SERV2	11.01	20.02	25.08	0.4	0.41	29.6	11.27	20.37	47.33
SERV3	10.77	18.62	24.67	0	0	0	10.8	18.75	24.72
REST1	13.2	33.56	42.6	0	1.96	58.75	13.86	36.19	84.58
REST2	14.17	26.18	31.99	0	0	0.46	14.19	26.38	33.31
RETAIL1	13.48	28.89	36.93	0	9.52	74.73	13.38	36.78	89.77
RETAIL2	11.74	23.62	28.81	0	0	0.04	11.81	23.41	29.64
RETAIL3	5.2	10.45	16.6	0	0	0	6	11.35	16.1
ACCOM1	10.06	**42.12**	**55.37**	0	2.55	30.6	9.76	45.26	84.05
ACCOM2	13.07	24.65	32.27	**2.65**	24.18	42.54	15.84	43.13	63.11
HC1	12.43	20.95	26.14	0	0.96	4.44	10.98	21.05	31.57
HC2	**21.52**	33.76	41.43	0	0	2.21	**21.34**	35.24	44.62
HC3	20.59	35.03	41.96	0	0.01	0	20.22	34.78	42.64
UTIL	16.95	27.95	33.05	0	0.55	3.75	16.8	27.3	35.40
CONST1	13.88	21.27	25.28	0.03	6.4	**97.14**	12.99	25.81	**97.7**
CONST2	12.7	21.22	26.83	0.07	0.25	16.77	12.82	21.27	39.98
CONST3	8.32	15.74	20.78	0	0.06	0.37	7.85	15.27	20.96
MANUF2	14.03	23.7	29.68	0	0.01	6.36	14.12	23.9	34.24
AG2	7.9	17.4	20.95	0	0	10.25	8.35	16.4	28.8
AG3	15.15	23.9	30.15	0	0.25	0.5	15.3	22.55	30.1

Note: The economic sectors are deaggregated by the hazard and economic zones: Zone 1: ocean front, Zone 2: central, and Zone 3: inland. For example, HS3 refers to the housing sector located in Zone 3. The bold values correspond to the highest capital stock loss for each recurrence interval. For a definition of sectors, see footnote in Table 3. The number in front of the label for each sector indicates the corresponding economic zone.

Table 9. Example of spatial CGE results for hazards with the 500-year recurrence interval

		Earthquake		Tsunami		Earthquake + tsunami	
		500-year		500-year		500-year	
Resilience metrics	Zone	Amount of loss	Percentage loss	Amount of loss	Percentage loss	Amount of loss	Percentage loss
Total employment (person)	—	248	6.30	57	1.40	299	7.50
	Zone 1	89	6.5	16	1.2	105	7.7
	Zone 2	121	6.0	30	1.5	147	7.3
	Zone 3	37	7.1	11	2.1	47	8.9
Domestic supply ($M)	—	204.3	13.9	31.7	2.2	232.7	15.8
	Zone 1	130.4	17.6	22.5	3.0	151.6	20.4
	Zone 2	54.1	9.8	8.1	1.5	60.5	11.0
	Zone 3	19.8	10.9	1.0	0.6	20.6	11.3

definition of building functionality in the vulnerability analysis to aid decision makers in making informed decisions.

As broader applications, results in this paper can be used by the community decision makers and policymakers to make informed decisions for increasing community resilience of vulnerable communities to natural hazards. In addition, the model can be used to quantify the effect of different mitigation strategies, other than seismic retrofit, to provide better insight for emergency planners and decision makers. Although this paper considered the impact of the CSZ on the city of Seaside, the methodology is generalizable to other communities with different natural hazards, such as hurricanes and tornados.

Appendix. Spatial Losses Deaggregated by Economic Zones

Tables 8 and 9 present spatial losses, including capital stock and CGE results. Table 8 shows the capital stock losses for different economic sectors deaggregated by the hazards and economic zones, in which the sectors are ordered based on Table 3 to facilitate the comparison. The highest capital stock loss for each type of hazard and related recurrence interval is highlighted. As shown in Table 8, the capital losses of economic sectors were strongly dependent on the building type, hazard type, and economic zones. For example, given the seismic hazard, the capital stock losses in the housing sector (HS1, HS2, and HS3) were almost identical over different economic zones because most buildings in this sector are wood-frame structures. However, results indicate that buildings belonging to one economic sector but located in diffident zones can also experience different levels of capital stock losses. For example, given the 500-year seismic recurrence interval, ACCOM consists of two subsectors, ACCOM1 and ACCOM2, located in Zone 1 and 2, respectively. Although the aggregated capital stock loss of the ACCOM sector was estimated as 36.7%, the ACCOM1 subsector sustained nearly 17.5% loss higher than the ACCOM2 subsector (42.1% versus 24.6%). This difference in the capital stock loss was more substantial for the tsunami hazard. For instance, given the 500-year tsunami recurrence interval, whereas the total capital stock loss of the HS sector (housing sector) was about 16.5%, individual losses for HS1, HS2, and HS3 were 36.7%, 0.5%, and 0.0%, respectively.

Table 9 shows an example of CGE results disaggregated by the hazards and economic zones. To help understand the hazard's geographically heterogeneous economic impacts, this table illustrates the spatial CGE results for employment and domestic supply. The losses to employment and domestic supply resulted from business interruptions, which were determined by the level of capital stock damage. The CGE results provide that percentage losses for employment are similar across zones: the reason is that more workers were allocated in Zone 2 (1,933) compared to Zones 1 (1,287) and 3 (482). Therefore, job losses in Zone 1 were fewer than in Zone 2, even though Zone 1 was impacted more by the capital stock losses than Zone 2. Regarding domestic supply, Zone 1 suffered a larger decline in output. For instance, given the 500-year seismic recurrence interval, reductions in domestic supply in Zones 1, 2, and 3 were 17.6%, 9.8%, and 10.9%, respectively. The trends of results in domestic supply were consistent with those obtained from capital stock loss because damaged capital makes a lower amount of productive capital stock, leading to decrease economic activity and domestic supply.

Data Availability Statement

Data sets used in this study for the city of Seaside, Oregon, including built, natural, and social systems, are available in DesignSafe: https://www.designsafe-ci.org/data/browser/public/designsafe.storage.published/PRJ-3390. Other data and codes, including the CGE model, are available in the IN-CORE repository online, in accordance with funder data retention policies.

Acknowledgments

The Center for Risk-Based Community Resilience Planning is a NIST-funded Center of Excellence; the Center is funded through a cooperative agreement between the US National Institute of Standards and Technology and Colorado State University (NIST Financial Assistance Award Nos. 70NANB15H044 and 70NANB20H008). The findings and views expressed are those of the authors and may not represent the official position of the National Institute of Standards and Technology or the US Department of Commerce.

References

Abrahamson, N., N. Gregor, and K. Addo. 2016. "BC hydro ground motion prediction equations for subduction earthquakes." *Earthquake Spectra* 32 (1): 23–44. https://doi.org/10.1193/051712EQS188MR.

Ameri, M. R., and J. W. van de Lindt. 2019. "Seismic performance and recovery modeling of natural gas networks at the community level using building demand." *J. Perform. Constr. Facil.* 33 (4): 04019043. https://doi.org/10.1061/(ASCE)CF.1943-5509.0001315.

Amini, M., D. R. Sanderson, D. T. Cox, A. R. Barbosa, and N. Rosenheim. 2022. "Methodology to incorporate seismic damage and debris to evaluate strategies to reduce life safety risk for multi-hazard

earthquake and tsunami." *Nat. Hazard.* 1–36. https://doi.org/10.21203/rs.3.rs-1862973/v1.

Attary, N., H. Cutler, M. Shields, and J. W. van de Lindt. 2020. "The economic effects of financial relief delays following a natural disaster." *Econ. Syst. Res.* 32 (3): 351–377. https://doi.org/10.1080/09535314.2020.1713729.

Attary, N., J. W. van de Lindt, H. Mahmoud, and S. Smith. 2019. "Hindcasting community-level damage to the interdependent buildings and electric power network after the 2011 Joplin, Missouri, tornado." *Nat. Hazard. Rev.* 20 (1): 04018027. https://doi.org/10.1061/(ASCE)NH.1527-6996.0000317.

Bocchini, P., D. M. Frangopol, T. Ummenhofer, and T. Zinke. 2014. "Resilience and sustainability of the civil infrastructure: Towards a unified approach." *J. Infrastruct. Syst.* 20 (2): 04014004. https://doi.org/10.1061/(ASCE)IS.1943-555X.0000177.

Burns, P. O., A. R. Barbosa, M. J. Olsen, and H. Wang. 2021. "Multihazard damage and loss assessment of bridges in a highway network subjected to earthquake and tsunami hazards." *Nat. Hazard. Rev.* 22 (2): 05021002. https://doi.org/10.1061/(ASCE)NH.1527-6996.0000429.

CAFR (Comprehensive Annual Financial Report). 2017. *Comprehensive annual financial report for the fiscal year 2017*. Seaside, OR: City of Seaside.

Capozzo, M., A. Rizzi, G. P. Cimellaro, M. Domaneschi, A. R. Barbosa, and D. Cox. 2019. "Multi-hazard resilience assessment of a coastal community due to offshore earthquake." *J. Earthquake Tsunami* 13 (2): 1950008. https://doi.org/10.1142/S1793431119500088.

Cardenete, M. A., A. I. Guerra, and F. Sancho. 2012. *Applied general equilibrium*. Berlin: Springer.

Carey, T. J., H. B. Mason, A. R. Barbosa, and M. H. Scott. 2019. "Multihazard earthquake and tsunami effects on soil–foundation–bridge systems." *J. Bridge Eng.* 24 (4): 04019004. https://doi.org/10.1061/(ASCE)BE.1943-5592.0001353.

CEMHS (Center for Emergency Management and Homeland Security). 2020. *Spatial hazard events and losses database for the United States*. Phoenix: CEMHS, Arizona State Univ.

Chang, S., and M. Shinozuka. 2004. "Measuring improvements in the disaster resilience of communities." *Earthquake Spectra* 20 (3): 739–755. https://doi.org/10.1193/1.1775796.

Chen, Y., H. Park, Y. Chen, P. Corcoran, D. T. Cox, J. Reimer, and B. Weber. 2018. "Integrated engineering–economic model for the assessment of regional economic vulnerability to tsunamis." *Nat. Hazard. Rev.* 19 (4): 04018018. https://doi.org/10.1061/(ASCE)NH.1527-6996.0000307.

Chen, Z., A. Z. Rose, F. Prager, and S. Chatterjee. 2017. "Economic consequences of aviation system disruptions: A reduced-form computable general equilibrium analysis." *Transp. Res. Part A Policy Pract.* 95 (Jan): 207–226. https://doi.org/10.1016/j.tra.2016.09.027.

Clatsop County Assessment and Taxation Data. 2017. *Clatsop County assessment and taxation data*. Clatsop County, OR: Clatsop County Assessment and Taxation Data.

Cox, D. T., A. R. Barbosa, M. Alam, M. Amini, S. Kameshwar, H. Park, and D. Sanderson. 2022. *Seaside testbed data inventory for infrastructure, population, and earthquake-tsunami hazard*. Seattle, WA: DesignSafe-CI. https://doi.org/10.17603/ds2-sp99-xv89.

Cutler, H., M. Shields, D. Tavani, and S. Zahran. 2016. "Integrating engineering outputs from natural disaster models into a dynamic spatial computable general equilibrium model of Centerville." *Sustainable Resilient Infrastruct.* 1 (3–4): 169–187. https://doi.org/10.1080/23789689.2016.1254996.

Dixon, P., and M. T. Rimmer. 2002. *Dynamic general and equilibrium modelling for forecasting and policy: A practical guide and documentation of MONASH*. Bingley, UK: Emerald Group.

Ellingwood, B. R., H. Cutler, P. Gardoni, W. G. Peacock, J. W. van de Lindt, and N. Wang. 2016. "The Centerville virtual community: A fully integrated decision model of interacting physical and social infrastructure systems." *Sustainable Resilient Infrastruct.* 1 (3–4): 95–107. https://doi.org/10.1080/23789689.2016.1255000.

FEMA. 2013. *Tsunami methodology technical manual*. Washington, DC: FEMA.

FEMA. 2015. *HAZUS–MH 2.1 technical manual*. Washington, DC: FEMA.

Gall, M., K. A. Borden, C. T. Emrich, and S. L. Cutter. 2011. "The unsustainable trend of natural hazard losses in the United States." *Sustainability* 3 (11): 2157–2181. https://doi.org/10.3390/su3112157.

Gardoni, P., J. van de Lindt, B. Ellingwood, T. McAllister, J. S. Lee, H. Cutler, W. Peacock, and D. Cox. 2018. "The interdependent networked community resilience modeling environment (IN-CORE)." In *Proc., 16th European Conf. on Earthquake Engineering*, 18–21. Istanbul, Turkey: European Association for Earthquake Engineering.

Goldfinger, C., et al. 2012. *Turbidite event history—Methods and implications for holocene paleoseismicity of the Cascadia subduction zone*. Reston, VA: USGS.

Guidotti, R., H. Chmielewski, V. Unnikrishnan, P. Gardoni, T. McAllister, and J. W. van de Lindt. 2016. "Modeling the resilience of critical infrastructure: The role of network dependencies." *Sustainable Resilient Infrastruct.* 1 (3–4): 153–168. https://doi.org/10.1080/23789689.2016.1254999.

Heaton, T. H., and S. H. Hartzell. 1987. "Earthquake hazards on the Cascadia subduction zone." *Science* 236 (4798): 162–168. https://doi.org/10.1126/science.236.4798.162.

Joshi, G., and S. Mohagheghi. 2021. "Optimal operation of combined energy and water systems for community resilience against natural disasters." *Energies* 14 (19): 6132. https://doi.org/10.3390/en14196132.

Kameshwar, S., D. T. Cox, A. R. Barbosa, K. Farokhnia, H. Park, M. S. Alam, and J. W. van de Lindt. 2019. "Probabilistic decision-support framework for community resilience: Incorporating multi-hazards, infrastructure interdependencies, and resilience goals in a Bayesian network." *Reliab. Eng. Syst. Saf.* 191 (Nov): 106568. https://doi.org/10.1016/j.ress.2019.106568.

Kircher, C. A., and J. Bouabid. 2014. "New building damage functions for tsunami." In *Proc., 10th National Conf. in Earthquake Engineering*. Anchorage, AK: Earthquake Engineering Research Institute.

Lin, N., and E. Shullman. 2017. "Dealing with hurricane surge flooding in a changing environment. Part I: Risk assessment considering storm climatology change, sea level rise, and coastal development." *Stochastic Environ. Res. Risk Assess.* 31 (9): 2379–2400. https://doi.org/10.1007/s00477-016-1377-5.

Liu, F. 2014. "Projections of future US design wind speeds due to climate change for estimating hurricane losses." Ph.D. thesis, Dept. of Civil Engineering, Clemson Univ.

Lynett, P., T. Wu, and P. Liu. 2002. "Modeling wave runup with depth-integrated equations." *Coastal Eng.* 46 (2): 89–107. https://doi.org/10.1016/S0378-3839(02)00043-1.

Ma, L., P. Bocchini, and V. Christou. 2020. "Fragility models of electrical conductors in power transmission networks subjected to hurricanes." *Struct. Saf.* 82 (Jan): 101890. https://doi.org/10.1016/j.strusafe.2019.101890.

Masoomi, H., J. W. van de Lindt, and L. Peek. 2018. "Quantifying socioeconomic impact of a tornado by estimating population outmigration as a resilience metric at the community level." *J. Struct. Eng.* 144 (5): 04018034. https://doi.org/10.1061/(ASCE)ST.1943-541X.0002019.

Meyer, V., et al. 2013. "Assessing the costs of natural hazards—State of the art and knowledge gaps." *Nat. Hazards Earth Syst. Sci.* 13 (5): 1351–1373. https://doi.org/10.5194/nhess-13-1351-2013.

Modarres, M., M. Kaminskiy, and V. Krivtsov. 2016. *Reliability engineering and risk analysis: A practical guide*. Boca Raton, FL: CRC Press.

Newman, J. P., H. R. Maier, G. A. Riddell, A. C. Zecchin, J. E. Daniell, A. M. Schaefer, H. van Delden, B. Khazai, M. J. O'Flaherty, and C. P. Newland. 2017. "Review of literature on decision support systems for natural hazard risk reduction: Current status and future research directions." *Environ. Modell. Software* 96 (Oct): 378–409. https://doi.org/10.1016/j.envsoft.2017.06.042.

NRC (National Research Council). 1999. *The impacts of natural disasters: A framework for loss estimation*. Washington, DC: National Academy Press.

OSSPAC (Oregon Seismic Safety Policy Advisory Commission). 2013. *The Oregon resilience plan: Reducing risk and improving recovery for the next Cascadia earthquake and tsunami*. Salem, OR: OSSPAC.

Ouyang, M., and L. Duenas-Osorio. 2014. "Multi-dimensional hurricane resilience assessment of electric power systems." *Struct. Saf.* 48 (May): 15–24. https://doi.org/10.1016/j.strusafe.2014.01.001.

Ouyang, M., and Z. Wang. 2015. "Resilience assessment of interdependent infrastructure systems: With a focus on joint restoration modeling and analysis." *Reliab. Eng. Syst. Saf.* 141 (Sep): 74–82. https://doi.org/10.1016/j.ress.2015.03.011.

Park, H., M. Alam, D. T. Cox, A. R. Barbosa, and J. W. van de Lindt. 2019. "Probabilistic seismic and tsunami damage analysis (PSTDA) of the Cascadia subduction zone applied to Seaside, Oregon." *Int. J. Disaster Risk Reduct.* 35 (Apr): 101076. https://doi.org/10.1016/j.ijdrr.2019.101076.

Park, H., D. T. Cox, M. Alam, and A. R. Barbosa. 2017a. "Probabilistic seismic and tsunami hazard analysis conditioned on a megathrust rupture of the Cascadia subduction zone." *Front. Built Environ.* 3 (Jun): 32. https://doi.org/10.3389/fbuil.2017.00032.

Park, H., D. T. Cox, and A. R. Barbosa. 2017b. "Comparison of inundation depth and momentum flux-based fragilities for probabilistic tsunami damage assessment and uncertainty analysis." *Coastal Eng.* 122 (Apr): 10–26. https://doi.org/10.1016/j.coastaleng.2017.01.008.

PDNA (Post-Disaster Needs Assessment). 2010. *Haiti earthquake PDNA: Assessment of damage, losses, general and sectoral needs*. Washington, DC: World Bank.

Pilkington, S. F. 2019. "Integration of graphical, physics-based, and machine learning methods for assessment of impact and recovery of the built environment from wind hazards." Ph.D. dissertation, Dept. of Civil and Environment Engineering, Colorado State Univ.

PUMS (Public Use Microdata Sample). 2017. *ACS public use microdata sample (PUMS) overview*. Washington, DC: US Census Bureau.

QCEW (Quarterly Census of Employment and Wages). 2017. *Quarterly census of employment and wages*. Washington, DC: Bureau of Labor Statistics.

Rappaport, J., and J. D. Sachs. 2003. "The United States as a coastal nation." *J. Econ. Growth* 8 (1): 5–46. https://doi.org/10.1023/A:1022870216673.

Rong, Y., D. D. Jackson, H. Magistrale, and C. Goldfinger. 2014. "Magnitude limits of subduction zone earthquakes." *Bull. Seismol. Soc. Am.* 104 (5): 2359–2377. https://doi.org/10.1785/0120130287.

Roohi, M., J. W. van de Lindt, N. Rosenheim, Y. Hu, and H. Cutler. 2021. "Implication of building inventory accuracy on physical and socioeconomic resilience metrics for informed decision-making in natural hazards." *Struct. Infrastruct. Eng.* 17 (4): 534–554. https://doi.org/10.1080/15732479.2020.1845753.

Rose, A. 2004. "Defining and measuring economic resilience to disasters." *Disaster Prev. Manage.* 13 (4): 307–314. https://doi.org/10.1108/09653560410556528.

Rose, A., and S. Y. Liao. 2005. "Modeling regional economic resilience to disasters: A computable general equilibrium analysis of water service disruptions." *J. Reg. Sci.* 45 (1): 75–112. https://doi.org/10.1111/j.0022-4146.2005.00365.x.

Rose, A., and D. Lim. 2002. "Business interruption losses from natural hazards: Conceptual and methodological issues in the case of the Northridge earthquake." *Environ. Hazards* 4 (1): 1–14. https://doi.org/10.1080/23789689.2019.1681821.

Rose, A., I. S. Wing, D. Wei, and A. Wein. 2016. "Economic impacts of a California tsunami." *Nat. Hazard. Rev.* 17 (2): 04016002. https://doi.org/10.1061/(ASCE)NH.1527-6996.0000212.

Rosenheim, N., R. Guidotti, P. Gardoni, and W. G. Peacock. 2019. "Integration of detailed household and housing unit characteristic data with critical infrastructure for post-hazard resilience modeling." *Sustainable Resilient Infrastruct.* 6 (6): 385–401. https://doi.org/10.1080/23789689.2019.1681821.

Sanderson, D., D. T. Cox, A. R. Barbosa, and J. Bolte. 2022. "Modeling regional and local resilience of infrastructure networks following disruptions from natural hazards." *J. Infrastruct. Syst.* 28 (3): 04022021. https://doi.org/10.1061/(ASCE)IS.1943-555X.0000694.

Sanderson, D., D. T. Cox, and G. Naraharisetty. 2021a. "A spatially explicit decision support framework for parcel- and community-level resilience assessment using Bayesian networks." *Sustainable Resilient Infrastruct.* 7 (5): 531–551. https://doi.org/10.1080/23789689.2021.1966164.

Sanderson, D., S. Kameshwar, N. Rosenheim, and D. T. Cox. 2021b. "Deaggregation of multi-hazard damages, losses, risks, and connectivity: An application to the joint seismic-tsunami hazard at Seaside, Oregon." *Nat. Hazard.* 109 (2): 1821–1847. https://doi.org/10.1007/s11069-021-04900-9.

Schultz, M. T., and E. R. Smith. 2016. "Assessing the resilience of coastal systems: A probabilistic approach." *J. Coastal Res.* 321 (5): 1032–1050. https://doi.org/10.2112/JCOASTRES-D-15-00170.1.

Shoven, J. B., and J. Whalley. 1992. *Applying general equilibrium*. Cambridge, UK: Cambridge University Press.

Sun, W., P. Bocchini, and B. D. Davison. 2020. "Resilience metrics and measurement methods for transportation infrastructure: The state of the art." *Sustainable Resilient Infrastruct.* 5 (3): 168–199. https://doi.org/10.1080/23789689.2018.1448663.

Tirasirichai, C. 2007. "An indirect loss estimation methodology to account for regional earthquake damage to highway bridges." Ph.D. thesis, Dept. of Engineering Management, Univ. of Missouri-Rolla.

Titov, V. V., C. W. Moore, D. J. M. Greenslade, C. Pattiaratchi, R. Badal, C. E. Synolakis, and U. Kânoğlu. 2011. "A new tool for inundation modeling: Community modeling interface for tsunamis (ComMIT)." *Pure Appl. Geophys.* 168 (11): 2121–2131. https://doi.org/10.1007/s00024-011-0292-4.

US Census Bureau. 2020. "Table P1 total population by race. 2020 Census redistricting data (public law 94-171)." Accessed July 13, 2022. https://data.census.gov/cedsci/table?g=1600000US4165950&tid=DECENNIALPL2010.P1.

van de Lindt, J. W., et al. 2023. "The interdependent networked community resilience modeling environment (IN-CORE)." *Resilient Cities Struct.* 2 (2): 57–66. https://doi.org/10.1016/j.rcns.2023.07.004.

van de Lindt, J. W., B. R. Ellingwood, H. Cutler, P. Gardoni, J. S. Lee, D. Cox, and W. G. Peacock. 2019. "The structure of the Interconnected Networked Community Resilience Modeling Environment (IN-CORE)." In *Proc., 2nd Int. Conf. on Natural Hazards & Infrastructure*, 23–26. Athens, Greece: National Technical Univ. of Athens.

Wang, W., J. W. van de Lindt, B. Hartman, H. Cutler, J. L. Kruse, T. P. McAllister, and S. Hamideh. 2022. "Determination of individual building performance targets to achieve community-level social and economic resilience metrics." *J. Struct. Eng.* 148 (5): 04022045. https://doi.org/10.1061/(ASCE)ST.1943-541X.0003338.

Wang, W., J. W. van de Lindt, N. Rosenheim, H. Cutler, B. Hartman, J. S. Lee, and D. Calderson. 2021. "Effect of residential building wind retrofits on social and economic community-level resilience metrics." *J. Infrastruct. Syst.* 27 (4): 04021034. https://doi.org/10.1061/(ASCE)IS.1943-555X.0000642.

Wang, Y., N. Wang, P. Lin, B. Ellingwood, H. Mahmoud, and T. Maloney. 2018. "De-aggregation of community resilience goals to obtain minimum performance objectives for buildings under tornado hazards." *Struct. Saf.* 70 (1): 82–92. https://doi.org/10.1016/j.strusafe.2017.10.003.

Wiebe, D. M., and D. T. Cox. 2014. "Application of fragility curves to estimate building damage and economic loss at a community scale: A case study of Seaside, Oregon." *Nat. Hazard.* 71 (3): 2043–2061. https://doi.org/10.1007/s11069-013-0995-1.

Wood, N. J. 2007. *Variations in city exposure and sensitivity to tsunami hazards in Oregon*. Scientific Investigations Rep. No. 2007-5283. Washington, DC: USGS.

Wood, N. J., C. G. Burton, and S. L. Cutter. 2010. "Community variations in social vulnerability to Cascadia-related tsunami in the US Pacific Northwest." *Nat. Hazard.* 52 (Feb): 369–389. https://doi.org/10.1007/s11069-009-9376-1.

Zhang, Y., N. Yang, and U. Lall. 2016. "Modeling and simulation of the vulnerability of interdependent power-water infrastructure networks to cascading failures." *J. Syst. Sci. Syst. Eng.* 25 (1): 102–118. https://doi.org/10.1007/s11518-016-5295-3.

Zhou, L., and Z. Chen. 2021. "Are CGE models reliable for disaster impact analyses?" *Econ. Syst. Res.* 33 (1): 20–46. https://doi.org/10.1080/09535314.2020.1780566.